Publication Year	2021
Acceptance in OA@INAF	2023-09-13T11:06:49Z
Title	Electromagnetic Counterparts of Compact Binary Mergers
Authors	Stefano Ascenzi; Gor Oganesyan; Marica Branchesi; CIOLFI, RICCARDO
DOI	10.1017/S0022377820001646
Handle	http://hdl.handle.net/20.500.12386/34376
Journal	JOURNAL OF PLASMA PHYSICS
Number	87

1

Electromagnetic counterparts of compact binary mergers

Stefano Ascenzi [1,2,3,†], **Gor Oganesyan**[4,5], **Marica Branchesi**[4,5] **and**
Riccardo Ciolfi[6,7]

[1]INAF – Osservatorio Astronomico di Brera, Via E. Bianchi 46, I-23807 Merate, Italy

[2]Institute of Space Sciences (ICE, CSIC), Campus UAB, Carrer de Can Magrans s/n,
08193 Barcelona, Spain

[3]Institut d'Estudis Espacials de Catalunya (IEEC), Carrer Gran Capita 2–4, 08034 Barcelona, Spain

[4]Gran Sasso Science Institute, Viale F. Crispi 7, I-67100 L'Aquila (AQ), Italy

[5]INFN - Laboratori Nazionali del Gran Sasso, I-67100, L'Aquila (AQ), Italy

[6]INAF–Osservatorio Astronomico di Padova, Vicolo dell'Osservatorio 5, I-35122 Padova, Italy

[7]INFN–Sezione di Padova, Via Francesco Marzolo 8, I-35131 Padova, Italy

The first detection of a binary neutron star merger through gravitational waves and photons marked the dawn of multimessenger astronomy with gravitational waves, and it greatly increased our insight in different fields of astrophysics and fundamental physics. However, many open questions on the physical process involved in a compact binary merger still remain and many of these processes concern plasma physics. With the second generation of gravitational wave interferometers approaching their design sensitivity, the new generation under design study and new X-ray detectors under development, the high energy universe will become more and more a unique laboratory for our understanding of plasma in extreme conditions. In this review, we discuss the main electromagnetic signals expected to follow the merger of two compact objects highlighting the main physical processes involved and some of the most important open problems in the field.

---

1. Introduction

Gravitational waves (GWs) are perturbations of the spacetime propagating as waves at the speed of light. Although their interaction with matter is weak, extreme astrophysical processes are able to release through GWs such a huge amount of energy to be detectable by us. A class of such extreme astrophysical events is the merger of two compact objects – namely objects with a huge mass compressed in a very small volume – orbiting one around the other, where the emission of GWs removes angular momentum from the system shrinking the orbital separation between the two objects and leading to their

† Email address for correspondence: ascenzi@ice.csic.es

ultimate coalescence. Examples of compact objects are neutron stars (NSs) and black holes (BHs), for which a mass of the order of a solar mass is compressed within a radius of ∼10 km or less. It was indeed the merger of a system formed by two BHs, the first GW event ever detected, which was observed on 14 September 2015 by the LIGO and Virgo Scientific Collaborations (LVC) using the LIGO laser interferometers (Abbott *et al.* 2016*c*). The discovery was followed in subsequent years by other detections of BH–BH mergers (Abbott *et al.* 2016*a*,*b*, 2017*a*,*b*,*c*, 2018). On 17 August 2017 a different signal, originated by the coalescence of two NSs was observed by the LIGO and Virgo interferometer network (Abbott *et al.* 2017*d*). This detection was particularly interesting because, while for a BH–BH merger the emission of photons is not generally expected, the coalescence of an NS–NS system should be accompanied by a copious amount of electromagnetic (EM) radiation. Indeed, a few seconds after the merger, the satellites FERMI and INTEGRAL detected a flare of γ-rays in a direction of the sky compatible with the arrival direction of the GWs (Goldstein *et al.* 2017; Savchenko *et al.* 2017). A few hours later, ground-based telescopes identified the host galaxy of the GW source, NGC4993, by detecting the optical and near-infrared (NIR) counterpart (e.g. Chornock *et al.* 2017; Coulter *et al.* 2017; Drout *et al.* 2017; Pian *et al.* 2017; Shappee *et al.* 2017). A few days later the source was observed also in the X-ray and radio bands, and the observations continued for years after the GW event (Haggard *et al.* 2017; Troja *et al.* 2017; Alexander *et al.* 2018; D'Avanzo *et al.* 2018; Mooley *et al.* 2018; Ghirlanda *et al.* 2019; Hajela *et al.* 2020; Troja *et al.* 2020). This NS–NS merger, known as GW170817, which was observed through gravitational and multiwavelength EM radiation (Abbott *et al.* 2017*e*), marked the dawn of the new field of multimessenger astronomy with GWs.

The impact of the first GW-EM multimessenger detection has been wide. It contributed to answering many fundamental questions within the field of high-energy astrophysics and fundamental physics, such as the origin of a class of very energetic γ-ray emissions coming from distant galaxies known as short γ-ray bursts, and the existence of optical sources powered by the radioactive decay of heavy elements, known as kilonovae (or macronovae). The NS–NS mergers show themselves to be able to form collimated and very energetic outflows of matter, and to be important (likely dominant) formation sites of the heaviest elements in the universe such as gold, platinum, the lanthanides and the actinides. Moreover, this event furnished constraints, independent from those already extant, to the unknown equation of state of NS (Abbott *et al.* 2018) and the Hubble constant (Fishbach *et al.* 2019), extending the range of influence of multimessenger astronomy to the fields of quantum chromodynamics and cosmology. It is evident thus that the scientific potential of multimessenger astronomy is huge and covers many branches of physics.

Gravitational wave astrophysics and the physics governing the electromagnetic emission from GW sources are still in their early phase, and there is still an enormous theoretical effort required to be ready to interpret the multimessenger observations expected in the upcoming years. In this context, the physics of plasma plays a key role. The majority of the problems, which are not fully understood yet, require a deep knowledge of the dynamics of the plasmas in extreme regimes. Examples include the amplification of magnetic field during an NS–NS merger, the acceleration of particles responsible for the observed radiation and the role of magnetic reconnection in high-energy astrophysical processes. On the other hand, the universe constitutes a unique laboratory in which to get a better insight on the physics of plasma. It allows us to observe and study regimes of temperature, density and magnetic field that cannot be reached in laboratory experiments. In the near future, we expect great possibilities to explore these regimes due to the recently developed GW detectors and their next generation operating in synergy with innovative multiwavelength observatories, such as the Cherenkov Telescope Array (CTA) (Actis *et al.*

2011; Acharya *et al.* 2013), the proposed THESEUS mission (Amati *et al.* 2018; Stratta *et al.* 2018), the Vera C. Rubin Observatory (Ivezić *et al.* 2019), the European Extremely Large Telescope (ELT) (Gilmozzi & Spyromilio 2007), the Square Kilometre Array (SKA) (Carilli & Rawlings 2004) and more. This will boost considerably our understanding of the high-energy universe.

Here, we review the main EM counterparts of compact binary mergers – in particular NS–NS and NS–BH mergers – describing in a synthetic form the leading theoretical models and the most important open problems in the field. Our aim is not to give the reader a complete dissertation of the topic, but to provide a basic insight on the astrophysical processes involved in the coalescence of a compact binary system. For more detailed information, we will refer the interested reader to other reviews devoted to the specific topics summarized here (e.g. Piran 2004; Shibata & Taniguchi 2011; Bartos, Brady & Márka 2013; Berger 2014; Kumar & Zhang 2015; Rosswog 2015; Baiotti & Rezzolla 2017; Metzger 2017; Ciolfi 2018; Nakar 2019; Ciolfi 2020*b*).

This review is organized as follows. In § 2 we clarify some basic definitions useful for the reader. In § 3 we describe the dynamics of a compact binary merger. In § 4 we describe the process occurring after the merger, the EM emission they are responsible for and the open problems in the field. Finally, in § 5 we present our final remarks.

2. Basic definitions and constants

In this section we summarize some basic terms that are commonly used in astrophysics but which the plasma physics community may not be familiar with.

- 'Transient'. A transient is an astrophysical phenomenon with a short temporal duration compared with human time scales, namely it can last from seconds (or less) to years. For example, a supernova, which can be observable for months, is a transient, while a non-variable star, whose lifetime lies in the range 10^6–10^{10} years, is not.
- 'Metallicity'. An abundance of elements heavier than Helium (hence with atomic number greater than 2). In astrophysics generally we refer to these elements as metals.
- 'Compact object'. An astrophysical object with high mass compressed in a small volume. In particular, here compact object will refer only to NSs and (stellar-mass) BHs. An NS has a mass equal to 1–2 times the mass of the Sun within a radius of 10–13 km. Black holes treated in this review have a mass between a few times and 100 times the mass of the Sun. Their Schwarzschild radius increases linearly with the BH mass. For a BH of one solar mass, the Schwarzschild radius is ∼3 km.
- 'Lightcurve'. The lightcurve of a transient is the temporal evolution of the luminosity (or flux) of the source in a given frequency range. We refer to bolometric lightcuvre when the frequency range coincides with the whole EM spectrum.

Throughout the review the masses will be commonly expressed in terms of solar masses, where a solar mass corresponds to 1.989×10^{33} g and is indicated by the symbol $M_\odot$. Distances of astrophysical sources are expressed in multiples of parsec (pc), where 1 pc = 3.09×10^{18} cm.

3. Coalescence dynamics

The merger of an NS–NS or an NS–BH binary system is a complex event that requires full general relativistic magnetohydrodynamical (MHD) simulations to be properly studied. In fact, different initial orbital parameters and/or NS equation of state (EOS) can
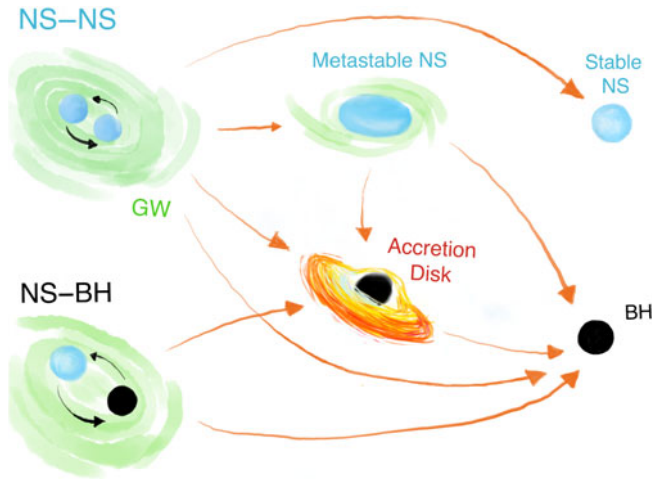
FIGURE 1. Different scenarios for an NS–NS and an NS–BH merger and the merger remnant. The EM radiation is expected when an accretion disk and unbound mass are left outside the merger remnant.

lead to a substantially different merger dynamics and in the case of an NS–NS merger even to different types of remnant objects. All the possible merger channels are summarized in figure 1. While an NS–BH merger can only result in the formation of a more massive BH, with an accretion disk if the NS is disrupted outside the BH's innermost stable circular orbit or without a disk in the opposite case, an NS–NS merger can result in the formation of a BH, a stable NS or, in most cases, a metastable NS collapsing to a BH after some time (e.g. Shibata, Taniguchi & Uryū 2005; Shibata & Taniguchi 2006; Baiotti, Giacomazzo & Rezzolla 2008; Rezzolla *et al.* 2010; Hotokezaka *et al.* 2011; Bauswein, Baumgarte & Janka 2013; Giacomazzo & Perna 2013; Ciolfi *et al.* 2017; Bernuzzi 2020). This last case can be divided in two subregimes: if the NS can be supported against collapse by uniform rotation the star is called supramassive neutron star (SMNS) and it remains stable as long as the rotation is not quenched. It is not clear for how long the collapse can be delayed and still result in a BH surrounded by a massive accretion disk (Margalit, Metzger & Beloborodov 2015; Ciolfi *et al.* 2019). If the star is instead so massive that can only be supported in the presence of differential rotation, it will collapse as soon as the NS core has acquired uniform rotation, which happens on time scales of $O(100 \, \text{ms})$. This object is named hypermassive neutron star (HMNS), and it likely leads to the formation of an accretion disk.

It is worth noting that during an NS–NS merger general relativistic MHD simulations show the development of the Kelvin–Helmholtz (KH) instability in the shear layer separating the two NS cores when they first come into contact. The generation of vortices amplifies the toroidal component of the magnetic field, even by one order of magnitude or more in the first few milliseconds (e.g. Kiuchi *et al.* 2015). Later on, further amplification is provided by magnetic field line winding and the magnetorotational instability (MRI) (Balbus & Hawley 1991; Duez *et al.* 2006; Siegel *et al.* 2013). Combined together, these processes are expected to increase the magnetic field strengths from premerger levels of the order of $B \sim 10^{12}$ G up to $B \sim 10^{15}$–10^{16} G (e.g. Price & Rosswog 2006; Giacomazzo *et al.* 2015). An NS with such a high magnetic field is usually called magnetar.[1] In this context,

---

[1] In a different context, magnetar refers to an NS whose persistent X-ray luminosity and bursting activity are powered by its strong magnetic field (see Mereghetti, Pons & Melatos (2015) for a recent review). Here, we simply call magnetar

an important issue is represented by the finite spatial resolution of the simulations, which is currently not sufficient to fully capture small-scale amplification mechanisms like the KH instability (Kiuchi *et al.* 2015). To overcome this limitation, effective subgrid amplification methods have been proposed (e.g. Giacomazzo *et al.* 2015; Carrasco, Viganò & Palenzuela 2020; Viganò *et al.* 2020).

A further important aspect to explore in compact binary mergers (CBMs) is the ejection of mass during the merger and post-merger phases. Part of the NS matter can expelled and become unbound (Davies *et al.* 1994; Rosswog *et al.* 1999). Tidal forces right before merger can cause partial disruption of the (two) NS(s), with material launched at mildly relativistic velocities on the orbital plane of the system (especially for binary systems characterized by objects of unequal mass). Moreover, once the accretion disk is formed, neutrino irradiation, nuclear recombination and magnetohydrodynamic viscosity can drive mass outflows from the disk (see § 4.3 for more details and references). In the specific case of NS–NS mergers, further ejection of matter in all directions (including polar regions) is produced by the shocks launched in the contact interface between the two stars when they touch. Moreover, the (meta)stable massive NS resulting from the merger can launch an additional baryon-loaded wind up to its collapse to a BH, if any (e.g. Ciolfi & Kalinani 2020). More details on these different ejecta components are given in §§ 4.3 and 4.4.

We conclude this section by briefly providing a qualitative description of the GW signal expected from a CBM. This signal can be divided into three phases: the inspiral, where the two objects are still distant and can be treated as point-like masses; the merger, where the objects come into contact and matter and finite size effects play an important role; and the ringdown, the final phase in which the newly formed compact object relaxes in a stationary configuration emitting an exponentially damped oscillating signal. The GW waveform of the inspiral part is a signal oscillating at a frequency of $f_{GW} = 2f_K$, where f_K is the Keplerian orbital frequency of the system which increases in time as the stars get closer. Its amplitude in turn follows the increase of frequency as $f_{GW}^{2/3}$. The resulting waveform is called chirp.[2]

Contrary to the inspiral signal, detailed simulations in general relativity are required to calculate the merger and post-merger GW signals, which strongly depend on the (still unknown) EOS describing NS matter at supranuclear densities. For NS-NS mergers, the post-merger signal (until collapse to a BH, if any) is typically dominated by a single frequency, related to the fundamental oscillation mode of the remnant. On longer time scales, if a long-lived SMNS or a stable NS is formed, it is expected to assume an ellipsoidal shape. This object will then further emit GWs at both $2f_{rot}$ and f_{rot} frequencies, where f_{rot} is the spin frequency. Since the object keeps spinning down and the amplitude of the signal is proportional to f_{rot}^2, the resulting waveform will be a sort of inverse chirp. The amplitude is also directly proportional to the remnant deformations with respect to axisymmetry around the spin axis, encoded by a quadrupolar ellipticity. Significant deformations can be expected, e.g. if the object has a strong internal magnetic field (e.g. Cutler 2002; Dall'Osso, Shore & Stella 2009; Ciolfi & Rezzolla 2013; Dall'Osso, Stella & Palomba 2018; Lander & Jones 2020).

4. Electromagnetic emission

In general, when at least one NS is involved in the merger, emission of photons is expected along with GWs. In figure 2 we illustrate the different EM emission components represented with a different colour. The only cases where the EM emission may be

---

an NS remnant with a magnetic field $B > 10^{14}$ G. In all the models described here, this huge magnetic field is used to extract the rotational energy of the star, which is the main reservoir of energy that powers the emission.

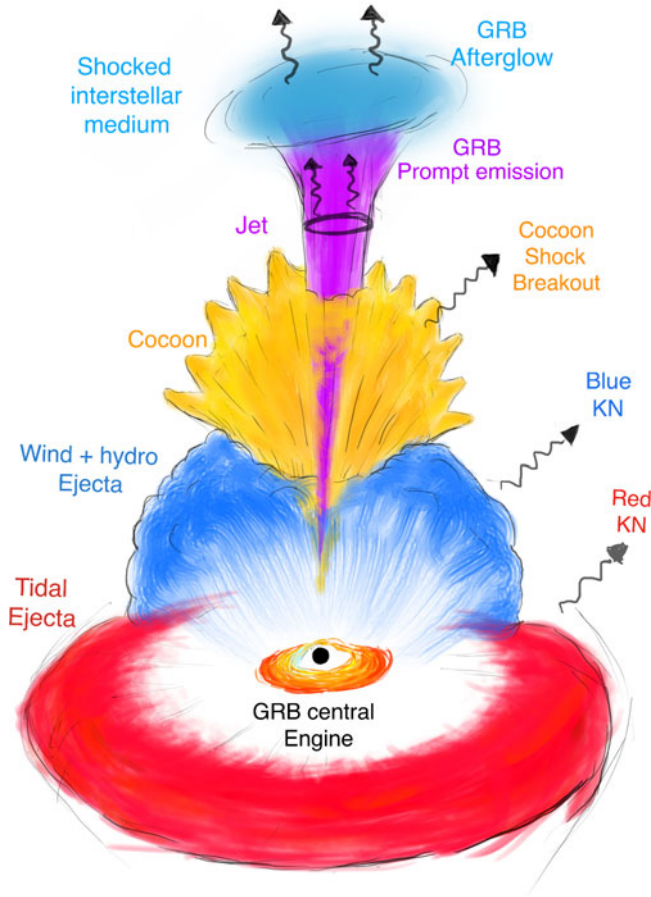[2]It is qualitatively similar to the chirp of a bird.

FIGURE 2. Artistic representation of the scenario following an NS–NS/NS–BH merger, when an accreting BH is formed. The red component denotes the tidal ejecta, the blue component the hydrodynamic and wind ejecta, the purple component the jet and the yellow component the matter of the ejecta heated by the jet (cocoon). The different components are not represented in scale.

suppressed are when a BH is promptly formed and leaves no accretion disk nor ejected material in NS binary mergers, and when the NS is swallowed by the BH without being disrupted in NS–BH mergers.

It is also possible that EM emission takes place even before the merger. This kind of emission, known as precursor emission, would occur irrespective of the final fate of the merger, namely it would be present even if a BH with no accretion disk results from the coalescence. Precursor emission will be discussed in § 4.1.

The remnant object resulting from the merger, either a differentially rotating massive NS or a BH surrounded by an accretion disk, is expected to launch a jet of relativistic matter[3] (purple component in figure 2) by physical processes which are, at present, not completely understood. The mechanisms to launch a jet are discussed later in § 4.2.1.

---

[3]This is commonly observed in other astrophysical sources consisting in accreting BHs, such as active galactic nuclei (Blandford, Meier & Readhead (2019) and references therein) and microquasars (Mirabel & Rodríguez (1999) and references therein).

Once formed, the jet drills through a dense circumburst medium, constituted by the material previously expelled by the merger (blue component in figure 2). During the jet crossing, the material in front of the jet's head is heated and moved aside, forming a hot structure called cocoon (yellow component in figure 2). The cocoon, in turn, exerts a transverse pressure which confines and further collimates the jet (Bromberg *et al.* 2011; Lazzati & Perna 2019; Salafia *et al.* 2019). If sufficiently energetic, the jet successfully emerges from the surrounding material (whose radius at this time is of the order $\sim 10^{10}$ cm), otherwise the jet can be choked. In the successful case, the jet travels until it becomes transparent at a radius of the order $\sim 10^{12}$ cm from the central engine (Piran 1999; Daigne & Mochkovitch 2002). At a distance range of 10^{13}–10^{16} cm the jet dissipates part of its kinetic energy powering an energetic gamma-ray radiation known as the GRB prompt emission. Alternatively, this emission can occur at the photosphere if the energy is dissipated below it. The internal dissipation mechanism is still poorly understood. Later on, the jet decelerates shocking the interstellar medium (in light blue in figure 2), powering a fading synchrotron emission from X-ray to radio called GRB afterglow. The GRB prompt and afterglow emission will be discussed in more detail in § 4.2. It is worth noticing that further EM radiation can originate from the cocoon when it breaks out from the circumburst medium and when it cools down by thermal emission. This kind of counterpart will not be discussed in the present review and we refer the interested reader to Nakar (2019).

The other component of the matter left outside after the CBM and unbound from the central remnant (blue and red components in figure 2) is rich of free neutrons and neutron-rich nuclei and represents an ideal site for the r-process nucleosynthesis of heavy elements (Lattimer & Schramm 1974; Symbalisty & Schramm 1982), whose radioactive decay heats up the material itself. This results in a thermal emission from the ejecta that generates a transient known as KN which will be discussed in more detail in § 4.3. It is also worth noting that the shock onto the interstellar medium of these mildly relativistic and subrelativistic outflows could in principle power a synchrotron emission expected to be observable in radio frequencies (Nakar & Piran 2011).

If the merger remnant is a very long-lived SMNS or a stable NS, the conditions required to form a magnetosphere can be met, leading to a magnetic dipole spindown radiation phase. Such emission would then energize the surrounding material (i.e. the previously emitted baryon-rich ejecta) powering an additional SDPT.

The EM counterparts of CBM briefly described here will be discussed in more detail in the following, with a special focus on the open problems in the field.

4.1. *Precursor emission*

The precursor emission is an EM signal preceding in time the peak of GW radiation, namely it is supposed to be emitted during the inspiral phase of the binary.

The general idea is that the signal is generated by the interaction between NS's magnetospheres (in case of an NS–NS system) or the orbital motion of a non-/weakly magnetized object through the magnetosphere of the companion. The latter framework, known as unipolar inductor has been studied analytically both for NS–NS (Vietri 1996; Hansen & Lyutikov 2001; Lai 2012; Piro 2012; Sridhar *et al.* 2020) and NS–BH systems (McWilliams & Levin 2011). In this framework the motion of the non-magnetized object through the companion magnetic field generates, due to Faraday's law, an electromotive force on the non-magnetized object. In this way a direct current circuit is established between the two stars, where the field lines behave like wires and the non-magnetized object as a battery. The accelerated charges may dissipate on the stellar surface or in the space between the two stars. In the latter case they may emit radio waves in a pulsar-like

fashion or trigger a pair cascade resulting in a wind emitting in the X-rays (Hansen & Lyutikov 2001; Piro 2012). Furthermore, shocks arising within the wind may generate an observable coherent radio emission through a synchrotron maser process (Sridhar *et al.* 2020).

The problem has been studied also with general relativistic resistive MHD (Palenzuela *et al.* 2013), special relativistic (Sridhar *et al.* 2020), force-free (Most & Philippov 2020) and particles-in-cell (Crinquand, Cerutti & Dubus 2019) simulations. These works allow us to appreciate the important role of magnetic reconnection in accelerating particles, which can further contribute to the emission.

Since this kind of emission takes place during the inspiral phase, its occurrence is insensitive of the merger product, namely it can be generated even in those cases in which no matter is left outside the newly formed BH. In these cases precursors represent the only possible EM counterpart. Although there is not a compelling observation for the above-described precursor yet, surveys able to detect them can provide candidate counterparts to be used for a coincident search of GWs.

4.2. γ-ray bursts

Gamma-ray bursts are highly energetic transient astrophysical sources of extragalactic origin, which have non-thermal spectra peaking at 10 keV–10 MeV. The γ-ray flaring activity of GRBs, which is called prompt emission, lasts typically less than a hundred of seconds and its lightcurve manifests a plethora of different morphologies and a time variability (time scale in which the fluxes vary by more than a factor of two) that can be of the order of few milliseconds (Walker, Schaefer & Fenimore 2000). Examples of typical prompt emission lightcurves are shown in figure 3, where the GRB data are taken by Burst and Transient Source Experiment (BATSE) onboard the Compton Gamma Ray Observatory (CGRO) and the lightcurves are expressed in terms of counts per seconds. The prompt emission is followed by the fainter afterglow across the whole EM spectrum which decay in time. An example of a typical afterglow lightcurve in different spectral ranges is shown in figure 4.

The duration of the prompt emission shows a bimodal distribution (Kouveliotou *et al.* 1993), with two peaks at 0.3 s and 30 s, which unveils the presence of two distinct GRB populations, also characterized by a different hardness of the spectrum: the population of short duration events with a harder spectrum, called short GRBs (SGRBs), and the population of long duration events with a softer spectrum, called long GRBs (LGRBs). The duration commonly used to separate short GRBs from long ones is 2 s in the BATSE energy range (20–600 keV).

From the γ-ray fluence and the distance of the source it is possible to calculate the isotropic equivalent energy of the burst, which can reach $E_{\gamma,\text{ISO}} \sim 10^{54}$ erg (Briggs *et al.* 1999; Abdo *et al.* 2009) for the most energetic GRBs. However, there is very strong evidence that the emission is not isotropic but beamed (Rhoads 1997, 1999; Frail *et al.* 2001). This reduces the value of the real energy by a factor equal to the solid angle of collimation $\theta^2/2$, limiting it in the range 10^{49}–10^{51} erg (Frail *et al.* 2001; Panaitescu & Kumar 2001; Bloom, Frail & Kulkarni 2003).

The variability time scales δt can give us further insight on the origin of this emission. It constrains the emitting region to a characteristic size of $l \sim c\delta t$. This size, together with the high luminosity and the fact that the emission lies in the γ-ray frequency range, leads to a source that should be so compact to be opaque to $\gamma - \gamma$ pair-production, which is in tension with the non-thermal nature of the observed spectra. This problem, known as the compactness problem (Ruderman 1975; Goodman 1986; Paczynski 1986; Piran 1995), is solved by requiring that the source is moving relativistically towards the observer with a
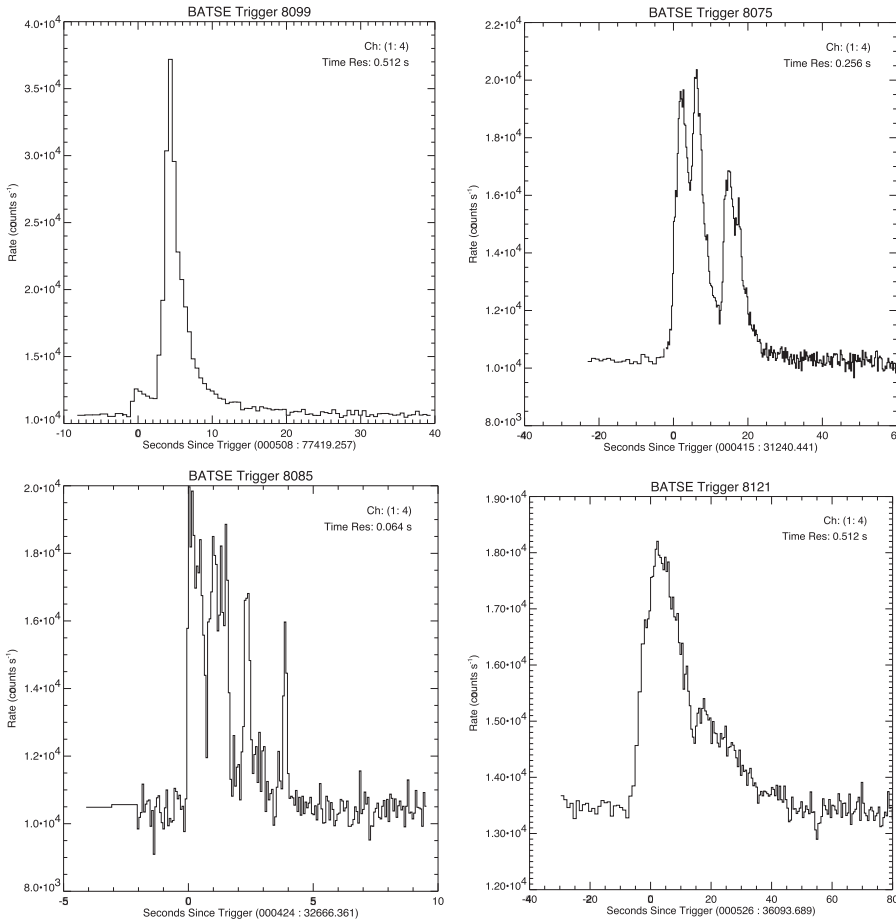
FIGURE 3. Examples of GRB prompt emission lightcurves ($E > 20$ keV) from the online BATSE catalogue (https://gammaray.nsstc.nasa.gov/batse/grb/lightcurve/).

Lorentz factor $\Gamma \geq 100$. This results in an increase of the true size of the source by a factor Γ^2, and in a blue-shift of the energy, which increases in the observer frame by a factor Γ (for a more detailed discussion of the compactness problem see Piran (2004)).

All the above considerations indicate that GRBs are generated by a collimated source moving relativistically towards the observer, the relativistic jet. The jet must be launched by some physical processes occurring within a short-living[4] object, which is usually referred to as a central engine, originated from a progenitor system.

The SGRBs and LGRBs have different progenitors. This was revealed by studies of the GRB energetics and redshift distribution (Nakar 2007), properties of their afterglow (Panaitescu, Kumar & Narayan 2001; Kann *et al.* 2011), their host galaxies (Berger 2009; Fong *et al.* 2013) and the recent observations of GWs.

A fraction of LGRBs optical afterglows show a late-time (in few weeks) bump due to an emergent associated type Ic supernova.[5] Thus, the LGRB afterglow observations

---

[4]Since GRBs do not repeat.

[5]Type Ic supernovae are supernovae whose spectrum is lacking of hydrogen lines (which are present in type II supernovae), silicon absorption line (present in type Ia supernovae) and helium lines (present in in type Ib supernovae). They are believed to be produced by core-collapse of massive stars which lose their hydrogen and helium envelopes prior to the explosion (Woosley & Bloom 2006).
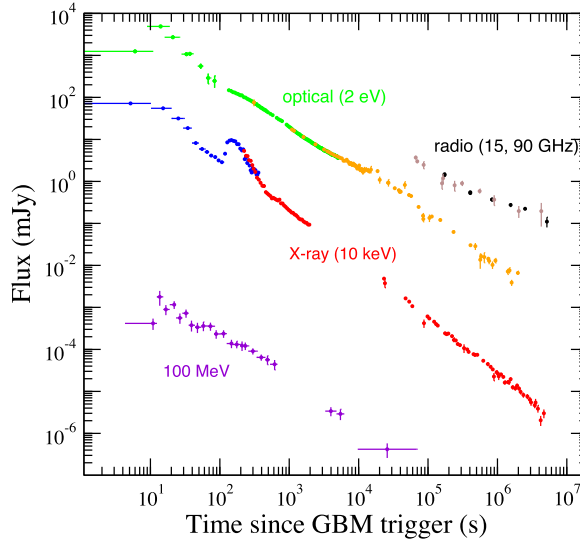
FIGURE 4. Example of a GRB afterglow in different spectral ranges. The data reported are for GRB 130427A afterglow (Panaitescu, Vestrand & Woźniak 2013). (Figure courtesy of Alin Panaitescu.)

empirically associate the sources of LGRBs with the death of massive stars (masses $M > 20M_\odot$) (Woosley & Bloom (2006) and references therein). The same conclusion comes from the study of their host galaxies which are typically irregular and star-forming galaxies (Fruchter *et al.* 2006). The LGRBs are preferentially located in the brightest spots of their host galaxies, i.e. highly star-forming regions where the massive stars are born. The supernovae signatures in LGRBs observations and the preferential location in actively star-forming regions, are strong evidence that massive stars are the progenitors of LGRBs.

On the other hand, most of the host galaxies of SGRBs show a relatively low star-formation rate (Fong, Berger & Fox 2010). When SGRBs are in star-forming galaxies, they are located in regions with lower star-formation rate and associate with an older star population with respect to LGRBs. This indicates that progenitors of SGRBs are older than those of LGRBs, since the region where they had formed is not active anymore or/and they had enough time to move away from their birth place. Astrophysical events satisfying all the required characteristics to be progenitors of SGRBs are the mergers of NS–NS or NS–BH binaries (Blinnikov *et al.* 1984; Paczynski 1986; Eichler *et al.* 1989). The first strong observational evidence to identify their progenitors came from the coincident detection of the first GW signal from the merger of NS–NS, GW170817, by the advanced LIGO and Virgo interferometers and the SGRB named GRB 170817A by the γ-ray detectors FERMI-GBM and INTEGRAL (Abbott *et al.* 2017*e*; Goldstein *et al.* 2017; Savchenko *et al.* 2017). Together with the multiwavelength observations spanning more than two years, which demonstrated the presence of a relativistic jet, this proved that the merger of two NS (in this specific case of total mass of $2.74^{+0.04}_{-0.01}$ M$_\odot$) can give rise to SGRBs.

Both core-collapse of a massive star and CBM involving NS are able to generate GRBs by forming either a temporary accretion disk around the remnant BH or a massive (meta)stable NS. These remnant systems are potentially able to power a relativistic jet via different mechanisms, and thus they are considered the most plausible GRB central engines. The internal dissipation of the jet energy at $R_\gamma \sim 10^{13}$ cm–10^{16} cm produces the
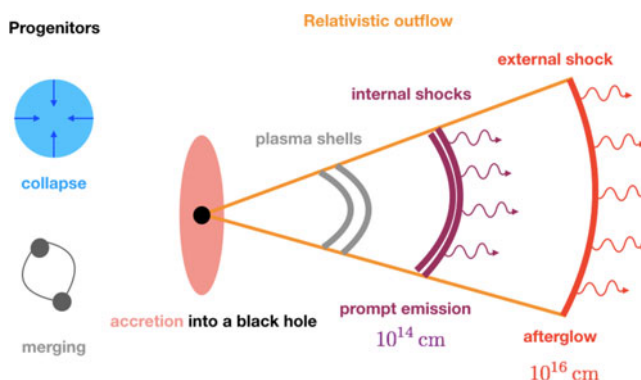
FIGURE 5. Pictorial representation of the basic model of the GRB: the core-collapse of a massive star or the coalescence of an NS–NS (or NS–BH) leads to the formation of an accreting BH, which launches an ultrarelativistic outflow in a form of a jet. Internal dissipation of the jet's kinetic energy through shocks produces the prompt emission in the keV–MeV range. The forward shock of the jet with ambient medium forms the afterglow radiation observed in the X-ray, optical and radio bands.

observed short-duration (10^{-3}–10^3 s) prompt emission seen in the keV–MeV energy range (Meszaros, Rees & Papathanassiou 1994; Rees & Meszaros 1994; Daigne & Mochkovitch 1998; Piran 1999) or, alternatively, the jet energy can be dissipated below the photosphere ($R \sim 10^{12}$ cm) and released at the photosphere (e.g. Rees & Mészáros 2005; Pe'er 2008; Beloborodov 2010; Lazzati *et al.* 2013; Bhattacharya & Kumar 2020).

The deceleration of the jet in the surrounding medium gives rise to the long-lived afterglow observed in the X-ray, optical and radio bands (Paczynski & Rhoads 1993; Mészáros & Rees 1997*a*; Sari, Piran & Narayan 1998). The characteristic physical size of the afterglow emitting region is $R_{\mathrm{aft}} \sim 10^{16}$–$10^{17}$ cm. The sketch of the basic model of the GRB phenomenon is shown in figure 5.

Since SGRBs originate from CBMs, they are the main objective of the present review. Nevertheless, various aspects discussed in the following apply also to the case of LGRBs.

4.2.1. *Central engine of short GRBs*

One of the fundamental unresolved questions in the GRB physics lies in the identification of the powerhouse of the relativistic jet (see, e.g. Ciolfi (2018) for a more extensive review). The proposed scenarios as the central engine of GRBs need to satisfy some minimal physical requirements.

One of them is the ability to power a jet with bulk Lorentz factors of order $\Gamma \geq 100$. This implies that the formed jet should contain a small number of baryons, otherwise their large inertia will prevent the fast motion (Shemi & Piran 1990). Moreover, highly variable light curves of the prompt emission suggest a discontinuous release of energy. As mentioned before, the main candidate that satisfies the above requirements is the hyperaccretion of a stellar mass BH, accreting at a rate $\dot{M} = 1$ $M_\odot$ s^{-1} (Woosley 1993). This rate is very high and exceeds by several orders of magnitude the Eddington limit, above which the feedback of radiation released by the accretion is strong enough to sweep off the infalling material hampering in this way the accretion. This limit in GRBs can be overcome because the disks are thought to be in a peculiar accretion regime, named neutrino-dominated accretion flow, where due to the high density and pressure,photons are trapped inside the matter and the neutrino emission dominates the disk cooling (see Liu, Gu & Zhang (2017),

for a recent review). Alternatively, a magnetar in fast rotation (periods of milliseconds) can power the relativistic jet via its rotational energy (Usov 1992).

The duration of the prompt emission is a further constraint on the nature of the central engine. While the prompt emission lasts for less than two seconds, we can observe late-time X-ray plateaus and/or flares (at 10^3–10^4 s) (Nousek *et al.* 2006; O'Brien *et al.* 2006; Zhang *et al.* 2006; Chincarini *et al.* 2007; Falcone *et al.* 2007). If we interpret these as a continuation of the energy output from the central engine (Rees & Mészáros 1998), then the central engine needs to be very long-lived and/or reactivated at such late times (e.g. Dai & Lu 1998; Zhang & Mészáros 2001; Yu, Cheng & Cao 2010).

In the case of an accreting BH central engine, the latter can power the jet by different mechanisms. The most discussed are the neutrino–antineutrino annihilation process (Goodman, Dar & Nussinov 1987; Eichler *et al.* 1989; Zalamea & Beloborodov 2011) and the Blandford–Znajek (BZ) mechanism (Blandford & Znajek 1977). The first mechanism is based on the fact that in the hottest inner part of the accretion disk, neutrino cooling is expected to become very efficient. When this happens, the annihilation of neutrino and antineutrino pairs above the disk should lead to the formation of an expanding fireball (electron–positron plasma mixed with photons). An estimate of the expected luminosity of the jet in this scenario comes from the power of neutrino–antineutrino annihilation and it is $\sim 10^{52}$ erg s^{-1} for a 3 M$_\odot$ black hole with an accretion rate $\dot{M} \sim 1$ M$_\odot$ s^{-1} (Zalamea & Beloborodov 2011). It is worth noticing that, in contrast, photon–photon pair production is not an available mechanism because of the above-mentioned regime of GRB's disks, in which photons are trapped and only neutrinos and antineutrinos are able to escape. The second mechanism, currently favoured, consists of extracting the rotational energy of a Kerr BH through a strong magnetic field threading it, which is sustained by electric currents within the accretion disk.

The energy is transported away in the form of a Poynting flux flowing mainly along the BH's rotational axis. For such a Poynting flux to exist a non-zero toroidal component of the magnetic field is required along the axis.[6] The toroidal magnetic field is generated by a poloidal current, streaming along the poloidal field lines that behave as wires. The electric currents must be sustained by an electromotive force. This is provided by a purely general relativistic effect, namely the frame-dragging around a rotating mass. The frame-dragging applied to the poloidal magnetic field lines results in the appearance of an electric field providing the required electromotive force. It is possible to prove that inside the BH's ergosphere – a region outside the event horizon where the frame-dragging is so intense that even photons are dragged to corotate with the BH – in order to attain the screening of this electric field, the required above mentioned poloidal current cannot vanish (Komissarov 2004).

A rapidly rotating NS remnant, with a period of the order of few milliseconds and dipolar magnetic field strengths of the order $\sim 10^{15}$ G represents a viable alternative to the accreting BH as a machine for the production of a relativistic jet. This central engine is often called a millisecond magnetar. Note that this type of engine can only apply to the case of NS–NS mergers. In such a scenario, the NS remnant, characterized by strong differential rotation, gradually builds up a strong helical magnetic field structure along the spin axis and the corresponding magnetic pressure gradients accelerate a collimated outflow in such direction (Ciolfi 2020a). This magnetorotational mechanism will remain

---

[6]The Poynting flux is $S \propto E \times H$, where E and H are the electric and auxiliary magnetic fields. Faraday's law, along with axisymmetry and stationarity, guarantees that the electric field is purely poloidal. So to have a non-vanishing radial component of S along the axis, a toroidal component of the magnetic field is required.

active only so long as the differential rotation in the core of the NS remnant persists, which is typically limited to subsecond time scales.

Recent simulations showed that the neutrino–antineutrino annihilation mechanism is likely not powerful enough to explain SGRB energetics (Just *et al.* (2016) and Perego, Yasin & Arcones (2017*b*), but see Salafia & Giacomazzo (2020)), pointing in favour of the alternative magnetically driven jet formation. A number of numerical relativity simulations of NS–NS and NS–BH mergers including magnetic fields as a key ingredient studied the potential to form a SGRB jet in the accreting BH scenario (e.g. Rezzolla *et al.* 2011; Kiuchi *et al.* 2014; Paschalidis, Ruiz & Shapiro 2015; Kawamura *et al.* 2016; Ruiz *et al.* 2016) and in the magnetar scenario (only for NS–NS mergers; e.g. Ciolfi *et al.* (2017), Ciolfi *et al.* (2019) and Ciolfi (2020*a*)). While a final answer is still missing, the most recent results support the BH scenario, either by showing that an incipient jet could form in this case (Paschalidis *et al.* 2015; Ruiz *et al.* 2016) or by showing that the collimated outflow from a magnetar would most likely be insufficient to explain the energy and Lorentz factors of SGRBs (Ciolfi 2020*a*).[7]

4.2.2. *Jet acceleration*

Once the jet is formed, it must accelerate to ultrarelativistic velocity. How it happens is strongly connected to the nature of the jet. There exist two limiting cases: a hot internal-energy-dominated jet and a cold magnetic-energy-dominated jet.

The first case is the most explored scenario and is known as hot fireball model (Cavallo & Rees 1978; Goodman 1986; Paczynski 1986). The general idea beyond this framework is that the internal energy of the jet is converted into bulk kinetic energy, such that the temperature of the fireball decreases while the jet accelerates. If we use the typical observed prompt emission luminosity $L \sim 10^{52}$ erg s^{-1} and the variability time scale of 10^{-2} s, we can estimate the initial temperature of the ejecta as $T \sim (L/4\pi(c\delta t)^2 \sigma_B)^{1/4} \sim 2 \times 10^{10}$ K. At this high temperature photons are coupled with electron–positron pairs and baryons. Jets with a small enough number of baryons will undergo an adiabatic expansion while photons cool. Therefore, the initial energy of photons, electrons and positrons is transferred to protons. The acceleration of the jet continues until photons decouple from baryons (Shemi & Piran 1990; Piran 1999).

The photosphere can be defined as a surface at which the optical depth to the Thomson scattering (τ) is equal to 1. The optical depth is $\tau \sim n_p \sigma_T R/2\Gamma$, where R is the radius of the ejecta and n_p is the proton density in the outflow. The comoving proton density estimate comes by the proton flux in the jet $\dot{M}$ as $n'_p = \dot{M}/(4\pi R m_p c \Gamma)$. Defining the ratio between the radiation luminosity L and the baryonic load $\dot{M}$ as $\eta = L/\dot{M}c^2$ we can get the photosphere radius $R_{ph} = R(\tau = 1)$ as $R = L\sigma_T/8\pi m_p c^3 \eta \Gamma^2$. Its typical value is $R_{ph} \sim 6 \times 10^{12}$ cm (if we use $L \sim 10^{52}$ erg s^{-1}, $\eta \sim 100$ and $\Gamma \sim 100$) (Piran 1999; Daigne & Mochkovitch 2002). The parameter η is the test parameter for identification of the jet composition. If thermal emission from the fireball is observed in the prompt emission spectra, its temperature constrains η and we have knowledge of the initial form of the jet's energy. Unfortunately, we do not have significant observational claims on the thermal components in GRBs spectra to answer to this question.

---

[7]Recently, Mösta *et al.* (2020) reported the formation of a mildly relativistic collimated outflow from a massive NS remnant, also showing that the presence of neutrino radiation can lead to a more powerful outflow compared with the case without neutrino radiation. In their set of simulations, however, a strong ($B = 10^{15}$ G) dipolar magnetic field is superimposed by hand on the NS remnant at 17 ms after merger. This assumption, while having a major impact on the result, may not be realistic, which casts doubts on the conclusion that massive NS remnants would be able to launch powerful jets.

The alternative is a cold jet, dominated by the Poynting flux (as, for example, in the BZ mechanism). These kinds of jets can be accelerated by converting the magnetic energy in kinetic energy of the bulk flow. This can occur, for example, due to the adiabatic expansion of the outflow, where, in the axisymmetric and stationary limit, the conservation of mass and energy flux leads to the identification of the following conserved quantity:

$$\Gamma(1 + \sigma) = \text{const.,} \tag{4.1}$$

where σ is the plasma magnetization, defined as the ratio of Poynting flux and matter energy flux. This means that the magnetic energy stored in the jet is able, in principle, to accelerate the jet up to the maximum Lorentz factor of $\Gamma_{\max} = 1 + \sigma_0 \sim \sigma_0$, where $\sigma_0 \gg 1$ is the magnetization at the base of the jet. The acceleration is due to magnetic pressure gradients associated with the build-up of toroidal magnetic field via the winding of field lines caused by the fast and differentially rotating central engine. However, in order to reach $\Gamma_{\max}$, the head of the jet must be in causal contact with its base and this condition is reached as long as the flow is subsonic with respect to the speed of a fast-magnetosonic wave. Since this speed is approximately equal to the (relativistic) Alfvén velocity, whose corresponding Lorentz factor is $\Gamma_A = \sqrt{1 + \sigma}$, the condition $\Gamma = \Gamma_A$ sets a limit to the Lorentz factor of $\Gamma_{\mathrm{MS}} = (1 + \sigma_0)^{1/3} \sim \sigma^{1/3}$, reached at the distance R_{MS} from the central engine, which is known as magnetosonic point (Goldreich & Julian 1970). This value can be increased by a factor of $\theta_j^{-2/3}$, when the outflow is collimated within an angle θ_j due to the confinement exerted by the circumburst medium (the envelope of the progenitor star for LGRBs, the merger ejecta for SGRBs) (Tchekhovskoy, McKinney & Narayan 2009).

Above the magnetosonic point, the jet can be accelerated either due to adiabatic acceleration, when a non-stationary outflow in place of a time-independent jet is considered (Granot, Komissarov & Spitkovsky 2011), or by the dissipation of magnetic field due to magnetic reconnection, which converts magnetic energy into thermal energy and, in turn, into bulk kinetic energy, as in the hot fireball case (Drenkhahn 2002; Drenkhahn & Spruit 2002). It is worth noting that dissipation processes able to convert a Poynting flux dominated jet into a hot fireball can occur also where the interaction between the jet and the circumburst medium leads to the jet collimation, due to magnetic reconnection driven by unstable internal kink modes as appears in three-dimensional MHD simulations (Bromberg & Tchekhovskoy 2016).

For a more detailed description of the jet acceleration mechanisms we refer the reader to Kumar & Zhang (2015) and Zhang (2018).

4.2.3. *Jet dissipation mechanisms*

The observed prompt emission is originated by the dissipation of the jet's energy. The short variability of prompt emission lightcurves suggests that the dissipation occurs within the jet (internal dissipation) because the lightcurve produced by the forward shock of the jet into the surrounding ambient medium (external dissipation) is expected to be smoothed over a time scale which is longer than the total duration of the burst (see Fenimore, Madras & Nayakshin 1996; Sari & Piran 1997; Piran 1999, 2004).

The internal shocks model is widely used as a dissipation mechanism in baryon dominated jets (Rees & Meszaros 1994). In that model the central engine produces outflows with random Lorentz factors. The faster part of the outflow catches the slower one. The shocks propagate in both shells converting the bulk kinetic energy of the flow into the kinetic energy of the particle accelerating them, and also leading to a local magnetic field amplification (Heavens & Drury (1988) and Sironi & Spitkovsky (2011); for a review on the acceleration of particle in shocks we refer the interested reader to Sironi, Keshet

& Lemoine (2015*a*)). Relativistic electrons in magnetic field are expected to radiate their energy through synchrotron and inverse Compton processes.

The main advantage of the internal shocks model is the possibility of having a short variability time scale. For simplicity, let us consider that the central engine produces two shells (with bulk Lorentz factors Γ_1 and Γ_2) with time difference δT. If the first shell is slower $\Gamma_1 < \Gamma_2$ then they collide at time t_{coll} defined by $v_1 t_{\text{coll}} = v_2(t_{\text{coll}} - \delta T)$ (where v_1 and v_2 are the shells' velocities). The radius at which shells collide is $R_{\text{coll}} = t_{\text{coll}} v_1 \sim 2c\Gamma_1 \delta T \kappa$ where $\kappa = \Gamma_2/\Gamma_1$. The observed variability tracks then the intrinsic central engine variability. However, the efficiency of internal shocks dissipation, which depend on the velocity difference between the two shells, is very low (approximately 20 % or lower) (Kobayashi, Piran & Sari 1997; Daigne & Mochkovitch 2002) and it represents one of the main issues of this model (but see Beniamini, Nava & Piran (2016)). Moreover, it was realized that the magnetization of the jet should be relatively low, i.e. $\sigma \sim 0.01$–0.1, otherwise the shocks will be suppressed (Sironi, Petropoulou & Giannios 2015*b*).

Alternatively, the prompt emission can be released at the photosphere, from subphotospheric dissipation (e.g. Rees & Mészáros 2005; Pe'er 2008; Beloborodov 2010; Lazzati *et al.* 2013; Bhattacharya & Kumar 2020). The subphotospheric dissipation can proceed through different mechanisms. One example is radiation dominated shocks, where the dissipation is controlled by photon scattering (e.g. Beloborodov (2017); see also Levinson & Nakar (2020) for a recent review about the topic). Another mechanism involves the turbulence within the jet, which transfer the kinetic energy of the flow to plasma particles, if the turbulence cascade reaches the microscopic scales, or directly to the radiation, in case turbulence cascade is damped at larger scales by bulk Compton scattering (Zrake, Beloborodov & Lundman 2019). Furthermore, if free neutrons are present, nuclear collision can constitute another important dissipation channel (Beloborodov 2017).

In the case of a Poynting flux dominated jet the basic dissipation mechanism, as already mentioned in the previous section, is the magnetic reconnection. During the reconnection the magnetic energy is dissipated to accelerate the charges, which then radiate through different emission processes (e.g. synchrotron emission). Particle acceleration can proceed also through a Fermi mechanism. This occurs when the particle scatters through the magnetic islands produced due to tearing instabilities in reconnection events, and moving close to the Alfvén speed (for acceleration of particles in reconnection layers see Spruit, Daigne & Drenkhahn (2001), Drenkhahn & Spruit (2002), Sironi & Spitkovsky (2014), Sironi *et al.* (2015*b*) and Petropoulou *et al.* (2019)). Moreover, tearing instability is also fundamental for enhancing the rate of reconnection events (for reviews on tearing instability see,e.g. Loureiro *et al.* (2012) and Comisso *et al.* (2016)).

In GRBs magnetic reconnection can be triggered by internal shocks, as proposed by Zhang & Yan (2011) in their Internal-collision-induced Magnetic Reconnection and Turbulence (ICMART) model. In the ICMART model the shock between shells endowed by ordered magnetic field (generated by the winding of magnetic field line in proximity of the central engine) cause a tangling of the field line, which favours magnetic reconnection on a length scale much smaller than the transverse size of the jet. Moreover, during the reconnection process, the plasma is accelerated and this further distorts the field lines, triggering further reconnection processes in a cascade fashion. The charges accelerated toward the observer radiate through a synchrotron process, and this should generate the γ-ray radiation constituting the GRB prompt emission. The distance from the central engine at which the dissipation occurs in the Zhang & Yan (2011) model is rather large, of the order of $\sim 10^{16}$ cm, however, the millisecond observed variability can be attained

considering that not the entire jet, but small regions of it, switch on independently.[8] Contrary to the internal shock model described at the beginning of this section, the ICMART model has a very high radiative efficiency.

4.2.4. *Afterglow*

As mentioned before, the deceleration of the jet in the surrounding medium gives rise to a long-lived emission, called afterglow, observed in radio frequencies, optical, X-ray, GeV and very recently also at TeV energies (Abdalla *et al.* 2019; MAGIC Collaboration *et al.* 2019). The characteristic radius, measured from the central engine, at which the deceleration, and thus the afterglow, occurs is $R_{\rm aft} \sim 10^{16}$–10^{17} cm.

The afterglow theory was developed before the first afterglow had been observed. It predicted an emission with a temporal power-law fading $t^{-\alpha}$ in a wide range of frequencies after the deceleration time (defined as the time at which the jet Lorentz factor halves). Here α depends on the power-law index p of the distribution of the emitting charges (see discussion below) and $\alpha \sim 1$ for expected values of p (Paczynski & Rhoads 1993; Mészáros & Rees 1997b; Sari *et al.* 1998). This prediction has been confirmed by the first afterglow observations (mainly in the optical band).[9] However, later observations with the Neil Gehrels Swift Observatory, (hereafter Swift), show that the X-ray lightcurve departures from the simple power-law behaviour , in a substantial fraction of events. The X-ray lightcurves show features like flares and a long-lasting plateau phase, whose origin is, at present, not clearly understood. This open question will be addressed in more detail in § 4.2.5.2.

The afterglow photons arises from the dissipation of the outflow kinetic energy. The supersonic flow of plasma interacts with the ambient developing a forward shock, where particles are accelerated by the Fermi acceleration mechanism (Fermi 1949) and magnetic field is amplified, likely due to the Weibel instability (Weibel 1959). In such a process, charged particles repeatedly cross the shock front gaining an energy proportional to the velocity of the shock front and forming a population of accelerated particles with a power-law distribution of Lorentz factor $N_\gamma \propto \gamma^{-p}$, where the index p is the power-law index of the distribution, expected to assume a value $p \sim 2.5$. These charges then radiate via a synchrotron process, generating the observed emission (Sari *et al.* 1998).

Along with the forward shock crossing the ambient medium, a reverse shock, propagating backward through the afterglow is expected to form if the jet, at this distance, is not strongly magnetized (i.e. $\sigma \ll 1$) (Meszaros & Rees (1993) and Sari & Piran (1999); see also Kumar & Zhang (2015) for a review).

As long as the outflow is in relativistic motion, the radiation, emitted isotropically in the rest frame, is beamed within an angle $\theta_{\rm beam} \sim \Gamma^{-1}$ in the observer frame. While the jet decelerates and Γ drops, the beaming angle increases and a wider portion of the emitting surface becomes visible to the observer. When $\theta_{\rm beam} \geq \theta_j$ the entire emission surface becomes visible to the observer, which means that there are no more debeamed photons that can be revealed by a further increase in $\theta_{\rm beam}$ and the flux start to drop faster, as $\sim t^{-2}$, in the whole EM spectrum (Rhoads 1999). This achromatic feature, known as jet break, has been one of the strongest pieces of evidence pointing towards the collimated nature of GRB outflows, and, when observed, the time at which it occurs allows us to measure the jet collimation angle θ_j (Sari, Piran & Halpern 1999). This information, in

---

[8]In GRB models this feature is often refer to as 'mini-jet' (Kumar & Piran 2000; Narayan & Kumar 2009).

[9]Actually, the first afterglows have been observed in X-rays, but the observations occurred at very late time from the GRB prompt, due to the large uncertainty γ-ray instrument in localizing the source along with the small field of view and the large time of repointing of X-ray telescopes.

turn, is fundamental in measuring the true energetic of the γ-ray prompt emission (Frail *et al.* 2001).

4.2.5. *Open problems*

In this section we address two of the principal open problems of GRBs: the physics behind the prompt emission spectra and the origin of the afterglow X-ray lightcurve.

4.2.5.1. Prompt emission: the mystery of the GRB spectra. The prompt emission spectrum indicates that the radiative processes are non-thermal. In particular, most of the observed GRB spectra are modelled as two power laws smoothly connected at the peak energy in the flux spectrum (in units of erg cm^2 s^{-1}) (Band *et al.* 1993; Preece *et al.* 1998; Frontera *et al.* 2000; Ghirlanda, Celotti & Ghisellini 2002). The power-law tail above the peak energy $\propto E^{-0.5}$, well resolved for the brightest GRBs, is prolonged in the energy range from hundreds of keV to sub-GeV range. It clearly supports the idea that the GRB spectrum most probably originates from a power-law distributed population of charged particles (i.e. $dN/d\gamma \propto \gamma^{-p}$, where γ is their random Lorentz factor), e.g. electrons accelerated in shocks (Rees & Meszaros 1994; Piran 1999).

The most straightforward process that could efficiently release the energy of charged electrons into the radiation is the synchrotron mechanism, which works both in the magnetic reconnection and internal shock dissipation scenarios. Therefore, the leptonic synchrotron radiation model used to interpret the prompt emission fits the general paradigm of the internal dissipation of the jet. Its main advantage is to explain the non-thermal nature of the observed GRB spectra by invoking a single and efficient radiative process.

In a simple scenario, a population of accelerated electrons are injected in a single shot into the emitting region with a given averaged magnetic field B. This idealization is representative of the internal shocks scenario, where the collision between two shells produce shocks which propagate into each of the shells resulting in the charged particles acceleration and in the amplification of the pre-existing magnetic field. While the physical system seem to be oversimplified, the synchrotron model has a solid prediction of the spectral index of the prompt emission below its peak energy, independent from the exact shape of the accelerated particles. The reason resides in the spectrum of the single particle, which is characterized by a power-law segment, growing as $\propto E^{4/3}$, followed at higher energy by an exponential cutoff. When a power-law distribution of the emitters is considered, the low energy spectrum is dominated by the contribution of the particles with the lowest γ resembling a single particle spectrum with the typical $E^{4/3}$ behaviour. Above the peak instead, the spectrum is given by the envelope of the peaks of the single particle spectra with different γ, such that the shape of the spectrum is a power law with a slope dependent on p. The lowest γ of the particle distribution do not coincide in general with the lowest γ of the initial distribution, which we call γ_m, because the charges lose energy by synchrotron emission at a rate $\propto \gamma^2$. After a certain time the emitters will populate states with $\gamma_c < \gamma < \gamma_m$ with a distribution like $dN/d\gamma \propto \gamma^2$, where γ_c is a minimum Lorentz factor determined by the cooling, and the states above γ_m with $dN/d\gamma \propto \gamma^{-p}$. The spectrum generated by such a distribution is a power law $\propto E^{4/3}$ below E_c (characteristic synchrotron energy for a particle with $\gamma = \gamma_c$), a power law $\propto E^{1/2}$ between E_c and E_m (same for E_c for $\gamma = \gamma_m$) and a power law $\propto E^{1-p/2}$ above E_m (Rybicki & Lightman 1986; Sari *et al.* 1998; Ghisellini 2013).

The main assumption here was that the electrons' cooling time via synchrotron losses t_c is much shorter than the dynamical time scale of the emitting region t_R (i.e. $t_c \gg t_R$), or alternatively, the integration time of the observed spectrum. This assumption is a

requirement for an efficient radiation of the energy deposited in the electron population. It was shown, that the above-mentioned scenario, known as fast cooling regime is the expected regime in the internal shocks model (Ghisellini, Celotti & Lazzati 2000). In this regime, the break at E_m occurs in the hard X-rays, while the break at E_c occurs at very low frequencies (e.g. radio). Thus, from X-ray to γ-ray the spectrum is expected to be a broken power-law with a single break at E_m.

The crisis of this scenario rises from the comparison of the low-energy photon indices with the expectation from the fast cooling regime of the synchrotron radiation. While the fast cooling regime predicts a spectrum of $\propto E^{1/2}$ below the peak energy, the typical observed spectra return $\propto E$ (Tavani 1996; Cohen *et al.* 1997; Crider *et al.* 1997; Preece *et al.* 1998). Steeper spectra are also observed. Even more, there is some number of GRB spectra that are steeper than the steepest possible low-energy tail predicted in the synchrotron radiation model, namely $\propto E^{4/3}$ (see, e.g. Acuner, Ryde & Yu 2019; Yu, Dereli-Bégué & Ryde 2019).

This problem has been widely discussed in the literature. The proposed solutions can be classified into two types: models which invoke emission mechanisms different than synchrotron radiation, and models which propose modifications to the basic synchrotron scenario. Among the first class of models, we recall scenarios invoking reprocessed emission, i.e. via Comptonization below the GRB fireball reaches its transparency, mixed thermal plus non-thermal processes and inverse Compton reprocessing of softer photon field (e.g. Liang *et al.* 1997; Blinnikov, Kozyreva & Panchenko 1999; Rees & Mészáros 2005; Giannios 2006; Pe'er 2008; Beloborodov 2010; Chhotray & Lazzati 2015; Vurm & Beloborodov 2016; Bhattacharya & Kumar 2020). For the second class of models (studies that consider synchrotron radiation above the photosphere), effects producing a hardening of the low-energy spectral index have been invoked, such as (1) effect of an energy dependent inverse Compton radiation (Klein–Nishina regime) (Derishev, Kocharovsky & Kocharovsky 2001), or self-absorption effect (Lloyd & Petrosian 2000), (2) effects of the magnetic field profile within the emitting region (Uhm & Zhang 2014), (3) the non-uniform small-scale magnetic fields (Medvedev 2000), (4) adiabatic cooling of electrons (Geng *et al.* 2018; Panaitescu 2019), (5) reacceleration and slow or balanced heating of the cooling electrons (Kumar & McMahon 2008; Asano & Terasawa 2009; Beniamini, Barniol Duran & Giannios 2018; Xu, Yang & Zhang 2018) (6) supercritical regime of hadronic cascades, i.e. a rapid energy conversion from protons to pions and muons triggered by the γ-ray photons (Petropoulou *et al.* 2014).

All these proposals suggest a specific configuration of the physical environments in which the observed emission is produced. Therefore, a clear identification of the radiative processes shaping the observed prompt emission spectra would be able to establish the physics of the relativistic jets responsible for GRBs, i.e. the jet composition and its dissipation processes. In spite of all theoretical efforts, there is still no consensus on the origin of the prompt emission.

In recent years, there were some additional observational and theoretical efforts aimed at resolving the dominant radiative processes responsible for the production of the GRB spectra. Among them, one intriguing discovery (Oganesyan *et al.* 2017) was made in the broadband studies of the prompt emission spectra. It turned out that the prompt emission spectra extended down to soft X-rays require the presence of an additional power-law segment. Once this break is included, the spectral indices become consistent with the predicted synchrotron emission spectrum in the fast cooling regime. Namely, the spectrum below the break energy (few keV) is consistent with the synchrotron spectrum from a single electron $\propto E^{4/3}$, while above they are in agreement with the fast cooling segment $\propto E^{1/2}$. These findings were later confirmed with a different instrumentation and with

the break energy at larger energies ($\sim$100 keV) (Ravasio *et al.* 2019). The synchrotron radiation model in a marginally fast cooling regime (Kumar & McMahon 2008; Daigne, Bošnjak & Dubus 2011; Beniamini & Piran 2013), i.e. when electrons cool down very little ($\gamma_c \sim \gamma_m$) in a single observed time-window, was confirmed by the direct application of the synchrotron model to the GRB data and by the early optical data, being consistent with $\propto E^{4/3}$ (Oganesyan *et al.* 2019). This scenario, suggested by the data, is quite challenging the single-shot acceleration model (where electrons are accelerated in a single episode) since it requires that electrons involved to produce the observed radiation, are somehow kept from efficient and fast cooling. Additionally, the parameter space of GRB emitting side is non-trivial. It requires that the radiation is produced in weak magnetic fields (B of few G), at relatively large radii ($R > 10^{16}$ cm) which contradicts the observed variability time scale of $t_{ang} \simeq R_\gamma/2c\Gamma^2 \sim 0.1$ s for a reasonable range of bulk Lorentz factors $\Gamma \sim 100$–300. Several modifications to the standard model, i.e. to the single-shot acceleration of electrons emitting from a surface of a jet with an angular size of $\theta >> 1/\Gamma$, could in principle provide this regime of radiation. Some models invoke continuous acceleration of electrons, and/or emission from large radii, invoking mini-jets to explain the short time variability (Narayan & Kumar 2009). However, mini-jets are likely to produce Comptonization,[10] which is not observed in the spectra. Another possibility is that there is a continuous heating/reacceleration of the electrons. If the acceleration time scale becomes comparable with the electrons' cooling time, then the synchrotron cooling frequency can be kept close to the peak energy, since particles are not allowed to cool down. This scenario was proposed in different dissipation models as a way to explain the observed spectral breaks in the X-rays (Beniamini *et al.* 2018; Gill, Granot & Beniamini 2020). The reacceleration of particles would require the presence of small-scale turbulence and/or the close by magnetic reconnection islands.

Recently Ghisellini *et al.* (2020) pointed out that is quite challenging to find a self-consistent and 'comfortable' parameter space for models invoking electrons as the synchrotron emitters and proposed a model in which the synchrotron emission it is due to protons. In this proton-synchrotron scenario, the observed marginally fast-cooling spectrum can be explained even at low emitting region size (e.g. $R \sim 10^{13}$ cm) and this can in principle solve the tension with the short time variability requirement.

At present the puzzle of the prompt emission still remains unsolved. We do not have a complete understanding of the initial composition of the relativistic jets of GRBs, and the dissipative mechanisms operating in them. It is quite intriguing to try to unveil a clear picture of how the GRB jets are formed, accelerate and dissipate prior to their interaction with the interstellar medium. Therefore, GRBs open an interdisciplinary laboratory, where the emerged magnetohydrodynamics, blast wave physics and plasma physics could find a platform to face the astrophysical observables.

4.2.5.2. Afterglow: the mystery of X-ray emission. Before the launch of the Swift satellite in 2004, GRB afterglows were mainly observed at relatively late times. The observed light curves were consistent with simple power-law in time, in agreement with the basic afterglow theory. However, the X-Ray telescope (XRT) on board the Swift shed new light onto the afterglow emission, revealing in the energy range of 0.3–10 keV complex behaviours which deviate from the simple blast wave deceleration profile (Tagliaferri *et al.* 2005; Nousek *et al.* 2006; O'Brien *et al.* 2006; Zhang *et al.* 2006).

---

[10]Because a big fraction of the whole GRB radiation is released in a region much smaller than the transverse size of the jet, so the radiation energy density is much higher than the case in which the entire surface emits (Ghisellini *et al.* 2020).

The earliest phase of the GRB X-ray emission consists of a steep decay. The flux temporal index α ($F \propto t^{-\alpha}$) is much larger than 2, which means that the emission fades much faster than predicted by the classical afterglow theory. Moreover, after the steep decay, several X-ray afterglows show a plateau phase characterized by a shallow ($\alpha \sim 0.5$) temporal decay that can last for hours. This phase can be followed by an abrupt flux suppression or by a new decay phase, which resembles the standard afterglow decay. This broken power-law behaviour observed in X-ray is inconsistent with the simple forward shock scenario. Afterglows presenting this feature are all but rare, since it is observed in $\sim 80\%$ of LGRB (Evans *et al.* 2009; Margutti *et al.* 2013; Melandri *et al.* 2014) and $\sim 50\%$ of SGRB (Rowlinson *et al.* 2013; D'Avanzo *et al.* 2014).

At late time ($> 10^3$ s), X-ray flares are often observed (Chincarini *et al.* 2010). Their temporal behaviour is similar to the prompt emission pulses. Therefore, if produced by internal energy dissipation, late-time X-ray flares require a reactivation of the GRB central engine.

The X-ray afterglow without the above features behaves as the standard theory predict; a decay phases with $\alpha \sim 1$, followed by a late-time fading with $\alpha \sim 2$ when the jet break occur.

The reason why the X-ray lightcurves behave so differently with respect to the lightcurves in the other energy ranges, while standard afterglow theory would predict a similar trend, is still an open issue in the field.

At present, the most understood feature is the steep decay, which is interpreted as the tail of the prompt emission and, as such, not related to the forward shock that powers the afterglow. This occurs because the emission region (approximated with a surface) is curved, and the photons emitted at the same time in different parts of the region reach the observer at different times. Considering the observer is supposedly aligned with the jet axis, the photons emitted close to the axis arrive earlier than those at higher latitude. Moreover, since the jet is expanding relativistically, the emission is beamed around the (radial) direction of motion. This means that photons emitted farther from the axis will be more debeamed from the observer line of sight with respect to those emitted close to the axis. Since the latter arrive before the former, the observer detects a flux rapidly fading in time. This effect, usually referred as high latitude emission (HLE) is able to account for the X-ray steep decay (Fenimore *et al.* 1996; Kumar & Panaitescu 2000).

On the contrary, the interpretation of X-ray plateaus is still debated. The more explored scenario invokes the presence of a long-lasting central engine, that remains active for hours after the GRB prompt emission (Rees & Mészáros 1998; Zhang *et al.* 2006). Since such a long period of activity is difficult to attain by an accreting BH (but see Kumar, Narayan & Johnson (2008)), millisecond magnetars have been proposed as a more suitable central engine candidate (Dai & Lu 1998; Zhang & Mészáros 2001). As already mentioned in § 4.2.1, a millisecond magnetar loses rotational energy via magnetic dipole spindown emission. This energy can be injected into the forward shock (external dissipation), or dissipated in proximity of the central engine (internal dissipation), sustaining in this way the X-ray emission.

A key feature of the magnetar central engine is that the magnetic dipole spindown emission is characterized by a constant luminosity up to a certain time, the characteristic spindown time when half of the energy is radiated, and then the luminosity is expected to decline as t^{-2}. Interestingly, for a millisecond magnetar, the spindown time scale is of the same order of magnitude of the typical plateau duration. Therefore, this well-defined temporal behaviour can straightforwardly account for the plateau in X-ray afterglow lightcurves and the successively decay phase. Moreover, if the magnetar is metastable, it may collapse into a BH when the spindown deprives it from centrifugal support.

When this happens, the energy outflow ceases abruptly, and if the X-ray radiation is generated by internal dissipation this can explain the sharp drop in flux sometimes observed (see, e.g. Troja *et al.* 2007; Sarin, Lasky & Ashton 2020). The magnetar model can successfully fit those GRB lightcurves that present a plateau (Lyons *et al.* 2010; Dall'Osso *et al.* 2011; Bernardini *et al.* 2012, 2013; Rowlinson *et al.* 2013) and can also account for an observed anticorrelation between plateau luminosity and duration (Dainotti, Cardone & Capozziello 2008).

Although promising, the magnetar central engine, as already explained, cannot guarantee the formation of the jet, due to the large number of baryons in the surrounding medium expected when a long-lived NS results from the merger. Since the jet is essential to explain both the prompt emission and the afterglow, this constitutes a very important issue for the magnetar model.

A different class of model that avoids the problems of the long-lasting central engines invokes a more refined description of the GRB jet. Beniamini *et al.* (2020) recently developed a model in which the X-ray plateau is generated by the forward shock driven by a structured jet,[11] when the observer is located slightly outside the jet axis. Another model has been proposed recently by Oganesyan *et al.* (2020), in which both the steep-decay and the plateau in X-ray can be explained by the prompt high-latitude emission when the jet is structured. Therefore, according to Oganesyan *et al.* (2020), the X-ray plateau is part of the tail of the prompt emission, while the forward shock is responsible for the optical and radio afterglow. This scenario is able to explain why the afterglow follows the standard theory in the optical band but often does not in the X-ray.

Concerning the X-ray flares, a late-time activity of the central engine is often invoked. This may be provided either by a magnetar central engine (Dai *et al.* 2006; Metzger *et al.* 2011; Bernardini *et al.* 2013) either by mechanisms similar to those responsible for the prompt emission or by dissipation of magnetic field as occurs in Galactic magnetars or by a BH accreting at late time (Perna, Armitage & Zhang 2006; Proga & Zhang 2006; Lee, Ramirez-Ruiz & López-Cámara 2009; Dall'Osso *et al.* 2017).

4.3. *Kilonova*

As was already stated, during an NS–NS or an NS–BH coalescence an amount of NS matter is expected to be unbound from the central remnant and ejected with mildly relativistic velocity. Since these expanding ejecta, as formed by NS decompressed matter, are neutron rich, they constitute a natural environment for r-process nucleosynthesis. This chain of nuclear reactions is characterized by the rapid capture of a number of free neutrons by neutron-rich nuclei, leading to the formation of very heavy elements. Due to the excess of neutrons, these elements are metastable and they eventually decay (mainly through β-decay) turning some neutrons into protons.[12] The radioactive decay of the newly synthesized heavy nuclei deposits energy within the ejecta via non-thermal particles such as γ-rays, α and β particles, and fission fragments, which then thermalizes efficiently and turns into ejecta internal energy. This energy excess is finally radiated away and produces the thermal transient which is commonly referred to as kilonova or macronova (Li & Paczyński 1998; Kulkarni 2005; Metzger *et al.* 2010; Metzger 2017).[13]

---

[11]A structured jet is a jet where the velocity and energy of the fluid have a non-constant profile with respect to the angular distance measured from the jet axis.

[12]Here the radioactive decay is slower than the rate of neutron capture. When the decay is instead faster, the nucleosynthesis occurs via the s-process (or 'slow' process).

[13]Some aspects of mass ejection and the possibility of an EM emission powered by the radioactive nuclides had been also anticipated in Blinnikov *et al.* (1990).

Within the context of a single component isotropic model (a model characterized by a single isotropic ejecta with uniform composition), it is possible to obtain an estimate for the main KN observational features, such as the peak luminosity, time at which the peak occur and brightness temperature at the peak. In this context the governing parameters are: the mass M_{ej}; the velocity v_{ej}; and the opacity k of the ejecta. A simple realistic model can be built using these three parameters. In fact, the first parameter, representing the total amount of matter undergoing radioactive decay, constitutes the 'fuel' of the KN, while all the three parameters determine the characteristic photon diffusion time scale. Taking into account a homogeneous composition and assuming that the peak of the emission occurs when the time scale of expansion equals the diffusion time scale (Arnett 1982), it is possible to obtain the following equations (Metzger *et al.* 2010):

$$
\left.
\begin{aligned}
t_{\text{peak}} &= \left(\frac{3kM_{ej}}{4\pi c v_{ej}}\right)^{1/2} \simeq 2.7 \text{ days} \left(\frac{M_{ej}}{10^{-2}\,M_\odot}\right)^{1/2} \left(\frac{v_{ej}}{0.1c}\right)^{-1/2} \left(\frac{k}{\text{cm}^2\,\text{g}^{-1}}\right)^{1/2} \\
L_{\text{peak}} &= M_{ej}\dot\epsilon_n(t_{\text{peak}}) \simeq 5\times10^{40}\frac{\text{erg}}{\text{s}}\epsilon_{\text{th}}\left(\frac{M_{ej}}{10^{-2}\,M_\odot}\right)^{0.35}\left(\frac{v_{ej}}{0.1c}\right)^{0.65}\left(\frac{k}{\text{cm}^2\,\text{g}^{-1}}\right)^{-0.65} \\
T_{\text{peak}} &= \left(\frac{L_{\text{peak}}}{4\pi\sigma R_{\text{peak}}^2}\right)^{1/4} \simeq 3460 \text{ K}\epsilon_{\text{th}}^{1/4}\left(\frac{M_{ej}}{10^{-2}\,M_\odot}\right)^{-0.17}\left(\frac{v_{ej}}{0.1c}\right)^{-0.09}\left(\frac{k}{\text{cm}^2\,\text{g}^{-1}}\right)^{-0.41}
\end{aligned}
\right\},
$$

(4.2)

where $\dot\epsilon_n$ is the specific radioactive heating rate, $\epsilon_{\text{th}} \leq 1$ is the thermalization efficiency and $R_p = v_{ej}t_p$ is the ejecta typical size at time t_p.

The opacity is determined by the composition of the matter. It depends on whether elements of the group of lanthanides are synthesized or not during r-process nucleosynthesis. These elements, due to the numerous transition lines in the optical bands, give rise to an opacity which can be even two order of magnitude higher than that of the iron group elements. If they are present, they dominate the net opacity of the ejecta (Barnes & Kasen 2013; Tanaka & Hotokezaka 2013). Their synthesis depends on the electron fraction of the ejected matter, which is defined as $Y_e \equiv n_p/(n_n + n_p)$ – where n_p and n_n are the proton and neutron number densities – and measures how much the matter is neutron rich. In particular, considering a threshold of $Y_e \simeq 0.25$, low Y_e ensures the synthesis of lanthanides, while high Y_e prevents it (Wu *et al.* 2016). Equations (4.2) show that the effect of increasing opacity is to shift the peak of the lightcurve at later time, to make the emission fainter, and to decrease its peak temperature making the transient redder in colour.

Figure 6(*a*) shows an example of a simple kilonova model outlined in Metzger (2017) characterized by mass of the ejecta $M_{ej} = 0.01\,M_\odot$, $v_{ej} = 0.1\,c$ and $k = 10\,\text{cm}^2\,\text{g}^{-1}$.

Although the single component model is instructive in understanding the qualitative impact of the parameters on the KN lightcurve and to have an indication of the brightness and spectral range of the emission (at an order of magnitude level), it is too simple for a comparison with the data. In fact, as it was anticipated in § 3, hydrodynamical simulations showed that in a CBM, several ejection mechanisms occur at different times leading to multiple ejecta components, with different mass, velocity and chemical composition (i.e. opacity). This prediction was confirmed by the detection of AT2017gfo, whose lightcurve is very hard to explain with a single component model (Perego, Radice & Bernuzzi 2017*a*; Pian *et al.* 2017; Tanaka *et al.* 2017).

In an NS–NS merger, an amount of matter of $M_{ej} \sim 10^{-3} - 10^{-2}\,M_\odot$ is expelled via dynamical mass ejection during the merger itself with a velocity of $v_{ej} \sim 0.1$–0.3 c and an
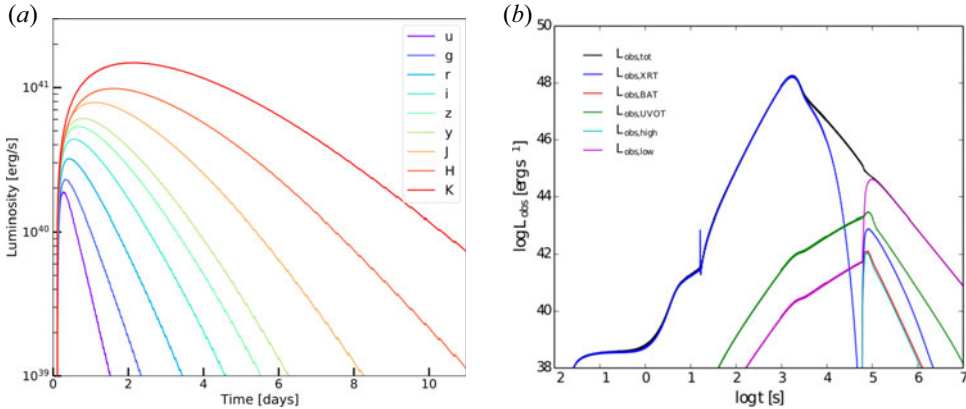
FIGURE 6. (*a*) The KN lightcurve in different photometric filters (optical and NIR) from a single component model characterized by $M_{ej} = 0.01$ M$_\odot$, $v_{ej} = 0.1\,c$ and $k = 10$ cm^2 g^{-1}. Lightcurves obtained with the code in https://github.com/mcoughlin/gwemlightcurves. (*b*) The SDPT lightcurve from the fiducial model in Siegel & Ciolfi (2016*b*) characterized by $M_{ej} = 5 \times 10^{-3}$ M$_\odot$ and $B = 10^{16}$ G. In this case the NS does not collapse. The black curve represents the bolometric luminosity, the dark blue curve is the lightcurve in the energy range of Swift-XRT (0.3–10 keV), the red curve in Swift-BAT range (15–150 keV), the green curve in Swift-UVOT range (170–650 nm). Light blue and purple curves represent lightcurves above BAT range and below UVOT range, respectively. Figure adapted from Siegel & Ciolfi (2016*b*).

electron fraction $Y_e \sim 0.05 - 0.4$. Tidal ejecta are responsible for the lower Y_e component and are located on the binary equatorial plane. Shock-driven ejecta, which cover the polar region, have higher Y_e, due to the fact that the matter is heated by the shocks and this leads to pair production and consequently to the capture of positrons by neutrons (Rosswog 2015). In the case of NS–BH merger only the tidal component is present and the unbound mass can reach $M_{ej} \sim 10^{-1}$ M$_\odot$ (Rosswog 2005; Foucart *et al.* 2014).

The presence of a (meta) stable massive NS, only for NS–NS mergers, would produce further mass outflow in the form of neutrino-driven (e.g. Dessart *et al.* 2009; Perego *et al.* 2014; Martin *et al.* 2015) and/or magnetically driven (e.g. Siegel, Ciolfi & Rezzolla 2014; Ciolfi *et al.* 2017; Ciolfi & Kalinani 2020) baryon-loaded winds, with a potentially high electron fraction due to the effect of neutrino irradiation from the NS itself, a mass of up to a few $\sim 10^{-2}$ M$_\odot$, and a velocity of $\sim$0.1–0.2 c (where the higher end can be achieved in the polar region in presence of a strong magnetic field; Ciolfi & Kalinani 2020).

Furthermore, after the collapse to a BH for NS–NS systems, or simply after merger for NS–BH systems, up to 40 % of the accretion disk mass can be ejected via MHD turbulence and neutrino heating within the disk itself (e.g. Siegel & Metzger 2018; Fernández *et al.* 2019). These disk wind ejecta are characterized by a wide range of electron fractions ($Y_e \sim$ 0.1–0.5) and low velocity $v_{ej} \lesssim 0.1$ c (e.g. Perego *et al.* 2014; Fernández *et al.* 2015; Martin *et al.* 2015; Wu *et al.* 2016; Siegel & Metzger 2017, 2018; Fujibayashi *et al.* 2018; Radice *et al.* 2018).

The presence of different matter components, with different mass, velocity and electron fraction, results in more complicated lightcurves with fast evolving bluer components (blue KN) and slower evolving redder components (red KN). Moreover, since each of the components have a different geometrical/angular distribution, the resulting KN lightcurve also depends on the orientation of the system with respect to the observer (e.g. Perego *et al.* 2017*a*; Wollaeger *et al.* 2018).

4.4. *Spindown-powered transients*

When the outcome of an NS–NS merger is another NS (stable or metastable), the newborn NS is expected to spin very fast with rotational periods of ∼1 ms, and to have a strong magnetic field – up to ∼10^{16} G in the interior – due to amplification mechanisms. During the first $O(100)$ ms the NS is hot and in differential rotation. In this phase, the strong neutrino irradiation and the gradient of magnetic pressure generated by the field winding due the action of differential rotation are responsible for a baryon-loaded wind (see also previous section). If the NS is a stable NS or SMNS it does not collapse when the core differential rotation is quenched, and it has a sufficient amount of time to lose its huge amount of rotational energy ($O(10^{52}$ erg)) through magnetic dipole spindown emission (Pacini 1967). The energy emitted at first as a Poynting flux is converted close to the source (by dissipation mechanisms not fully understood) in a electron–positron pair rich wind, analogous to a pulsar wind, expanding with relativistic velocities.[14] When the fast pulsar wind encounters the previously emitted and much slower baryon wind it drives a shock through it increasing its temperature and boosting its expansion. The thermal radiation from these hot expanding ejecta, gives origin to a spindown powered transient (SDPT) which is expected to be observable in X-ray, UV and optical bands (e.g. Yu, Zhang & Gao 2013; Metzger & Piro 2014; Siegel & Ciolfi 2016*a*,*b*).

So far, a compelling detection of this type of transients is still missing, although potential associations have been discussed in the literature (e.g. Ciolfi 2016; Xue *et al.* 2019). SDPTs are of particular interest since they are the only EM counterparts of CBM whose detection is a clear signature of the formation of a long-lived NS after the merger. The formation of such a type of NS would allow us to further constrain the NS EOS. Moreover, an SDPT detection would represent a secure way to distinguish a NS–NS merger from an NS–BH merger.

So far SDPT have been studied only through one-dimensional semianalytical approaches. These models consider a central NS, radiating via magnetic dipole emission, embedded in a PWN surrounded by an expanding spherical baryon wind. One of the first models of this kind was developed by Yu *et al.* (2013), who found a peak luminosity in the range 10^{44}–10^{45} erg s^{-1} occurring 10^4–10^5 s after the merger. Later Gao *et al.* (2015) applied this model to the SGRB GRB080503 to explain feature observed in its lightcurve. A similar model was developed by Metzger & Piro (2014), who provided a deeper focus on PWN physics in particular adding a self-consistent treatment of PWN opacity and baryon ejecta degree of ionization and albedo. They predict in this way a dimmer transient with respect to the Yu *et al.* (2013) model with peak luminosity in range 10^{43}–10^{44} erg s^{-1} peaking at 10^4–10^5 s after merger. Siegel & Ciolfi (2016*a*) advanced further the complexity of the treatment by including a relativistic dynamics, and starting the evolution from the baryon wind ejection, thus before the pulsar wind launching. In this way they followed three phases of the transient evolution: the baryon wind emitting phase; a second phase characterized by the pulsar wind and baryon wind interaction and the crossing of the shock through the latter; and a final phase in which the baryon wind expands under the pressure of an inner PWN. They predict that the transient peaks in the soft X-rays at ∼10^2–10^4 s after the merger, with a luminosity ranging in the interval 10^{46}–10^{48} erg s^{-1} (Siegel & Ciolfi 2016*b*). In figure 6(*b*) an example of an SPDT model from Siegel & Ciolfi (2016*b*) is shown.

---

[14]While this process has never been observed in an NS–NS merger scenario, this is what happens in the (less energetic) case of a pulsar wind nebula (PWN), which is a photon-pair plasma nebula powered by the magnetic spindown emission from an NS formed after a stellar core-collapse. See Gaensler & Slane (2006) for a review on the topic.

5. Final remarks

The merger of a binary system composed by two NSs or an NS and a BH is a powerful source of gravitational radiation that can also be followed by an intense emission of photons across the whole EM spectrum. So far, only one event of this kind, the NS–NS merger named GW170817, has been observed through these two different messengers. However, the information we gained by this single detection increased considerably our understanding in many different fields of astrophysics and fundamental physics.

The observation of a flash in γ-rays (Abbott *et al.* 2017*e*; Goldstein *et al.* 2017; Savchenko *et al.* 2017) along with a collimated outflow moving relativistically from the centre of explosion (Mooley *et al.* 2018; Ghirlanda *et al.* 2019) allowed us to confirm that (at least some) SGRBs are generated after an NS–NS merger. The multiwavelength observation of the afterglow showed that GRB relativistic jets are structured (Troja *et al.* 2017, 2018; Alexander *et al.* 2018; D'Avanzo *et al.* 2018).

The first NS–NS observation coincides also with the observation of a KN. The brightness and properties of the KN demonstrated that CBMs are favourable site of r-processes, which is the synthesis channel with whom the heaviest elements form in the universe.

The GW170817 has been also used to measure the Hubble constant (Fishbach *et al.* 2019), and the limits on the tidal deformability of the NSs have been used to constrain the dense matter EOS (Abbott *et al.* 2018).

Although the scientific outcome of GW170817 have been wide, many open questions concerning CBMs and their EM counterparts still remains unsolved. For example, at present, it is not clear how much the magnetic field can be amplified during an NS–NS merger (see, e.g. Ciolfi (2020*b*) for a recent review). The magnitude of the magnetic field, in turn, impacts the amount of matter ejected during the merger, the possibility to launch a jet and/or to form a magnetar as the result of the coalescence (and thus whether SDPTs occur in nature or not).

Concerning GRBs, many aspects of their physics are still not clear: Is a magnetar able to launch a GRB jet? Is the jet more similar to a hot fireball or to a cold Poynting flux dominated outflow? What are the dissipation mechanisms responsible for converting the jet kinetic energy in γ-ray radiation? What is the origin of the X-ray plateaus and X-ray flares often observed to occur in GRB afterglows? These are among the principal questions that astrophysicist need to address in the near future. Plasma physics is expected to play a key role in addressing them.

In the near future, the gravitational interferometers, the X-ray surveys such as eROSITA (Merloni *et al.* 2012), the wide field X-ray telescopes such as THESUS-SXI (Amati *et al.* 2018; Stratta *et al.* 2018), and the optical surveys such as the VEra Rubin Observatory (Ivezić *et al.* 2019), are going to provide us more and more joint GW-EM detections of CBMs. This represents a unique opportunity to unveil the physical mechanism at the base of the most energetic events in the universe and to study extreme environments characterized by intense gravity, strong magnetic fields, high densities and temperatures which cannot be reproduced in terrestrial laboratory. Observations of CBMs will allow us to get new insights into the physics of astrophysical plasmas.

Editor William Dorland thanks the referees for their advice in evaluating this article.

Declaration of interests

The authors report no conflict of interest.

Funding

REFERENCES

ABBOTT, B. P., ABBOTT, R., ABBOTT, T. D., ACERNESE, F., ACKLEY, K., ADAMS, C., ADAMS, T., ADDESSO, P., ADHIKARI, R. X., ADYA, V. B., *et al.* 2018 GW170817: measurements of neutron star radii and equation of state. *Phys. Rev. Lett.* **121** (16), 161101. arXiv:1805.11581.

ABBOTT, B. P., ABBOTT, R., ABBOTT, T. D., ABERNATHY, M. R., ACERNESE, F., ACKLEY, K., ADAMS, C., ADAMS, T., ADDESSO, P., ADHIKARI, R. X., *et al.* 2016*a* Binary black hole mergers in the first advanced LIGO observing run. *Phys. Rev.* **X6** (4), 041015. arXiv:1606.04856.

ABBOTT, B. P., ABBOTT, R., ABBOTT, T. D., ABERNATHY, M. R., ACERNESE, F., ACKLEY, K., ADAMS, C., ADAMS, T., ADDESSO, P., ADHIKARI, R. X., *et al.* 2016*b* GW151226: observation of gravitational waves from a 22-solar-mass binary black hole coalescence. *Phys. Rev. Lett.* **116** (24), 241103. arXiv:1606.04855.

ABBOTT, B. P., ABBOTT, R., ABBOTT, T. D., ABERNATHY, M. R., ACERNESE, F., ACKLEY, K., ADAMS, C., ADAMS, T., ADDESSO, P., ADHIKARI, R. X., *et al.* 2016*c* Observation of gravitational waves from a binary black hole merger. *Phys. Rev. Lett.* **116** (6), 061102. arXiv:1602.03837.

ABBOTT, B. P., ABBOTT, R., ABBOTT, T. D., ACERNESE, F., ACKLEY, K., ADAMS, C., ADAMS, T., ADDESSO, P., ADHIKARI, R. X., ADYA, V. B., *et al.* 2017*a* GW170104: observation of a 50-solar-mass binary black hole coalescence at Redshift 0.2. *Phys. Rev. Lett.* **118** (22), 221101. arXiv:1706.01812.

ABBOTT, B. P., ABBOTT, R., ABBOTT, T. D., ACERNESE, F., ACKLEY, K., ADAMS, C., ADAMS, T., ADDESSO, P., ADHIKARI, R. X., ADYA, V. B., *et al.* 2017*b* GW170608: observation of a 19-solar-mass binary black hole coalescence. *Astrophys. J.* **851** (2), L35. arXiv:1711.05578.

ABBOTT, B. P., ABBOTT, R., ABBOTT, T. D., ACERNESE, F., ACKLEY, K., ADAMS, C., ADAMS, T., ADDESSO, P., ADHIKARI, R. X., ADYA, V. B., *et al.* 2017*c* GW170814: a three-detector observation of gravitational waves from a binary black hole coalescence. *Phys. Rev. Lett.* **119** (14), 141101. arXiv:1709.09660.

ABBOTT, B. P., ABBOTT, R., ABBOTT, T. D., ACERNESE, F., ACKLEY, K., ADAMS, C., ADAMS, T., ADDESSO, P., ADHIKARI, R. X., ADYA, V. B., *et al.* 2017*d* GW170817: observation of gravitational waves from a binary neutron star inspiral. *Phys. Rev. Lett.* **119** (16), 161101. arXiv:1710.05832.

ABBOTT, B. P., ABBOTT, R., ABBOTT, T. D., ACERNESE, F., ACKLEY, K., ADAMS, C., ADAMS, T., ADDESSO, P., ADHIKARI, R. X., ADYA, V. B., *et al.* 2017*e* Multi-messenger observations of a binary neutron star merger. *Astrophys. J.* **848** (2), L12. arXiv:1710.05833.

ABBOTT, B. P., ABBOTT, R., ABBOTT, T. D., ABRAHAM, S., ACERNESE, F., ACKLEY, K., ADAMS, C., ADHIKARI, R. X., ADYA, V. B., AFFELDT, C., *et al.* 2018 GWTC-1: a gravitational-wave transient catalog of compact binary mergers observed by LIGO and virgo during the first and second observing runs. arXiv:1811.12907.

ABDALLA, H., ADAM, R., AHARONIAN, F., AIT BENKHALI, F., ANGÜNER, E. O., ARAKAWA, M., ARCARO, C., ARMAND, C., ASHKAR, H., BACKES, M., *et al.* 2019 A very high-energy component deep in the γ-ray burst afterglow. *Nature* **575** (7783), 464–467. arXiv:1911.08961.

ABDO, A. A., ACKERMANN, M., ARIMOTO, M., ASANO, K., ATWOOD, W. B., AXELSSON, M., BALDINI, L., BALLET, J., BAND, D. L., BARBIELLINI, G., *et al.* 2009 Fermi observations of high-energy gamma-ray emission from GRB 080916C. *Science* **323** (5922), 1688.

ACHARYA, B. S., ACTIS, M., AGHAJANI, T., AGNETTA, G., AGUILAR, J., AHARONIAN, F., AJELLO, M., AKHPERJANIAN, A., ALCUBIERRE, M., ALEKSIĆ, J., *et al.* 2013 Introducing the CTA concept. *Astropart. Phys.* **43**, 3–18.

ACTIS, M., AGNETTA, G., AHARONIAN, F., AKHPERJANIAN, A., ALEKSIĆ, J., ALIU, E., ALLAN, D., ALLEKOTTE, I., ANTICO, F., ANTONELLI, L. A., *et al.* 2011 Design concepts for the Cherenkov Telescope Array CTA: an advanced facility for ground-based high-energy gamma-ray astronomy. *Exp. Astron.* **32** (3), 193–316. arXiv:1008.3703.

ACUNER, Z., RYDE, F. & YU, H.-F. 2019 Non-dissipative photospheres in GRBs: spectral appearance in the Fermi/GBM catalogue. *MNRAS* **487** (4), 5508–5519. arXiv:1906.01318.

ALEXANDER, K. D., MARGUTTI, R., BLANCHARD, P. K., FONG, W., BERGER, E., HAJELA, A., EFTEKHARI, T., CHORNOCK, R., COWPERTHWAITE, P. S., GIANNIOS, D., *et al.* 2018 A decline in the X-Ray through radio emission from GW170817 continues to support an off-axis structured jet. *Astrophys. J. Lett.* **863**, L18. arXiv:1805.02870.

AMATI, L., O'BRIEN, P., GÖTZ, D., BOZZO, E., TENZER, C., FRONTERA, F., GHIRLANDA, G., LABANTI, C., OSBORNE, J. P., STRATTA, G., *et al.* 2018 The THESEUS space mission concept: science case, design and expected performances. *Adv. Space Res.* **62** (1), 191–244. arXiv:1710.04638.

ARNETT, W. D. 1982 Type I supernovae. I - analytic solutions for the early part of the light curve. *Astrophys. J.* **253**, 785–797.

ASANO, K. & TERASAWA, T. 2009 Slow heating model of gamma-ray burst: photon spectrum and delayed emission. *Astrophys. J.* **705** (2), 1714–1720. arXiv:0905.1392.

BAIOTTI, L., GIACOMAZZO, B. & REZZOLLA, L. 2008 Accurate evolutions of inspiralling neutron-star binaries: prompt and delayed collapse to a black hole. *Phys. Rev.* D **78** (8), 084033. arXiv:0804.0594.

BAIOTTI, L. & REZZOLLA, L. 2017 Binary neutron star mergers: a review of Einstein's richest laboratory. *Rep. Prog. Phys.* **80** (9), 096901. arXiv:1607.03540.

BALBUS, S. A. & HAWLEY, J. F. 1991 A powerful local shear instability in weakly magnetized disks. I. Linear analysis. *Astrophys. J.* **376**, 214.

BAND, D., MATTESON, J., FORD, L., SCHAEFER, B., PALMER, D., TEEGARDEN, B., CLINE, T., BRIGGS, M., PACIESAS, W., PENDLETON, G., *et al.* 1993 BATSE observations of gamma-ray burst spectra. I. Spectral diversity. *Astrophys. J.* **413**, 281.

BARNES, J. & KASEN, D. 2013 Effect of a high opacity on the light curves of radioactively powered transients from compact object mergers. *Astrophys. J.* **775**, 18. arXiv:1303.5787.

BARTOS, I., BRADY, P. & MÁRKA, S. 2013 How gravitational-wave observations can shape the gamma-ray burst paradigm. *Class. Quant. Grav.* **30** (12), 123001. arXiv:1212.2289.

BAUSWEIN, A., BAUMGARTE, T. W. & JANKA, H.-T. 2013 Prompt merger collapse and the maximum mass of neutron stars. *Phys. Rev. Lett.* **111** (13), 131101. arXiv:1307.5191.

BELOBORODOV, A. M. 2010 Collisional mechanism for gamma-ray burst emission. *MNRAS* **407** (2), 1033–1047. arXiv:0907.0732.

BELOBORODOV, A. M. 2017 Sub-photospheric shocks in relativistic explosions. *Astrophys. J.* **838** (2), 125. arXiv:1604.02794.

BENIAMINI, P., BARNIOL DURAN, R. & GIANNIOS, D. 2018 Marginally fast cooling synchrotron models for prompt GRBs. *MNRAS* **476** (2), 1785–1795. arXiv:1801.04944.

BENIAMINI, P., DUQUE, R., DAIGNE, F. & MOCHKOVITCH, R. 2020 X-ray plateaus in gamma-ray bursts' light curves from jets viewed slightly off-axis. *MNRAS* **492** (2), 2847–2857. arXiv:1907.05899.

BENIAMINI, P., NAVA, L. & PIRAN, T. 2016 A revised analysis of gamma-ray bursts' prompt efficiencies. *MNRAS* **461** (1), 51–59. arXiv:1606.00311.

BENIAMINI, P. & PIRAN, T. 2013 Constraints on the synchrotron emission mechanism in gamma-ray bursts. *Astrophys. J.* **769** (1), 69. arXiv:1301.5575.

BERGER, E. 2009 The host galaxies of short-duration gamma-ray bursts: luminosities, metallicities, and star-formation rates. *Astrophys. J.* **690** (1), 231–237. arXiv:0805.0306.

BERGER, E. 2014 Short-duration gamma-ray bursts. *ARA&A* **52**, 43–105. arXiv:1311.2603.

BERNARDINI, M. G., CAMPANA, S., GHISELLINI, G., D'AVANZO, P., BURLON, D., COVINO, S., GHIRLANDA, G., MELANDRI, A., SALVATERRA, R., VERGANI, S. D., *et al.* 2013 How to switch a gamma-ray burst on and off through a magnetar. *Astrophys. J.* **775** (1), 67. arXiv:1306.0013.

BERNARDINI, M. G., MARGUTTI, R., MAO, J., ZANINONI, E. & CHINCARINI, G. 2012 The X-ray light curve of gamma-ray bursts: clues to the central engine. *A&A* **539**, A3. arXiv:1112.1058.

BERNUZZI, S. 2020 Neutron stars merger remnants. e-prints. arXiv:2004.06419.

BHATTACHARYA, M. & KUMAR, P. 2020 Explaining GRB prompt emission with sub-photospheric dissipation and comptonization. *MNRAS* **491** (4), 4656–4671. arXiv:1909.07398.

BLANDFORD, R., MEIER, D. & READHEAD, A. 2019 Relativistic jets from active galactic nuclei. *ARA&A* **57**, 467–509. arXiv:1812.06025.

BLANDFORD, R. D. & ZNAJEK, R. L. 1977 Electromagnetic extraction of energy from Kerr black holes. *MNRAS* **179**, 433–456.

BLINNIKOV, S. I., IMSHENNIK, V. S., NADEZHIN, D. K., NOVIKOV, I. D., PEREVODCHIKOVA, T. V. & POLNAREV, A. G. 1990 Explosion of a low-mass neutron star. *Sov. Astron.* **34**, 595.

BLINNIKOV, S. I., KOZYREVA, A. V. & PANCHENKO, I. E. 1999 Gamma-ray bursts: when does a blackbody spectrum look non-thermal? *Astron. Rep.* **43** (11), 739–747. arXiv:astro-ph/9902378.

BLINNIKOV, S. I., NOVIKOV, I. D., PEREVODCHIKOVA, T. V. & POLNAREV, A. G. 1984 Exploding neutron stars in close binaries. *SvAL* **10**, 177–179.

BLOOM, J. S., FRAIL, D. A. & KULKARNI, S. R. 2003 Gamma-ray burst energetics and the gamma-ray burst hubble diagram: promises and limitations. *Astrophys. J.* **594** (2), 674–683. arXiv:astro-ph/0302210.

BRIGGS, M. S., BAND, D. L., KIPPEN, R. M., PREECE, R. D., KOUVELIOTOU, C., VAN PARADIJS, J., SHARE, G. H., MURPHY, R. J., MATZ, S. M., CONNORS, A., *et al.* 1999 Observations of GRB 990123 by the Compton gamma ray observatory. *Astrophys. J.* **524** (1), 82–91. arXiv:astro-ph/9903247.

BROMBERG, O., NAKAR, E., PIRAN, T. & SARI, R. 2011 The propagation of relativistic jets in external media. *Astrophys. J.* **740** (2), 100. arXiv:1107.1326.

BROMBERG, O. & TCHEKHOVSKOY, A. 2016 Relativistic MHD simulations of core-collapse GRB jets: 3D instabilities and magnetic dissipation. *Mon. Not. R. Astron. Soc.* **456** (2), 1739–1760.

CARILLI, C. L. & RAWLINGS, S. 2004 Motivation, key science projects, standards and assumptions. *New Astron. Rev.* **48** (11-12), 979–984. arXiv:astro-ph/0409274.

CARRASCO, F., VIGANÒ, D. & PALENZUELA, C. 2020 Gradient subgrid-scale model for relativistic MHD large-eddy simulations. *Phys. Rev. D* **101** (6), 063003. arXiv:1908.01419.

CAVALLO, G. & REES, M. J. 1978 A qualitative study of cosmic fireballs and gamma-ray bursts. *MNRAS* **183**, 359–365.

CHHOTRAY, A. & LAZZATI, D. 2015 Gamma-ray burst spectra and spectral correlations from sub-photospheric comptonization. *Astrophys. J.* **802** (2), 132. arXiv:1502.03055.

CHINCARINI, G., MAO, J., MARGUTTI, R., BERNARDINI, M. G., GUIDORZI, C., PASOTTI, F., GIANNIOS, D., DELLA VALLE, M., MORETTI, A., ROMANO, P., *et al.* 2010 Unveiling the origin of X-ray flares in gamma-ray bursts. *MNRAS* **406** (4), 2113–2148. arXiv:1004.0901.

CHINCARINI, G., MORETTI, A., ROMANO, P., FALCONE, A. D., MORRIS, D., RACUSIN, J., CAMPANA, S., COVINO, S., GUIDORZI, C., TAGLIAFERRI, G., *et al.* 2007 The first survey of X-ray flares from gamma-ray bursts observed by swift: temporal properties and morphology. *Astrophys. J.* **671** (2), 1903–1920. arXiv:astro-ph/0702371.

CHORNOCK, R., BERGER, E., KASEN, D., COWPERTHWAITE, P. S., NICHOLL, M., VILLAR, V. A., ALEXANDER, K. D., BLANCHARD, P. K., EFTEKHARI, T., FONG, W., *et al.* 2017 The electromagnetic counterpart of the binary neutron star merger LIGO/Virgo GW170817. IV. Detection

of near-infrared signatures of r-process nucleosynthesis with Gemini-South. *Astrophys. J. Lett.* **848**, L19. arXiv:1710.05454.

CIOLFI, R. 2016 X-ray flashes powered by the spindown of long-lived neutron stars. *Astrophys. J.* **829** (2), 72. arXiv:1606.01743.

CIOLFI, R. 2018 Short gamma-ray burst central engines. *Intl J. Mod. Phys.* D **27**, 1842004. arXiv:1804.03684.

CIOLFI, R. 2020*a* Collimated outflows from long-lived binary neutron star merger remnants. *Mon. Not. R. Astron. Soc. Lett.* **495** (1), L66–L70. arXiv:2001.10241.

CIOLFI, R. 2020*b* The key role of magnetic fields in binary neutron star mergers. *Gen. Relat. Gravit.* **52** (6), 59. arXiv:2003.07572.

CIOLFI, R. & KALINANI, J. V. 2020 Magnetically driven Baryon winds from binary neutron star merger remnants and the blue Kilonova of 2017 August. *Astrophys. J. Lett.* **900** (2), L35. arXiv:2004. 11298.

CIOLFI, R., KASTAUN, W., GIACOMAZZO, B., ENDRIZZI, A., SIEGEL, D. M. & PERNA, R. 2017 General relativistic magnetohydrodynamic simulations of binary neutron star mergers forming a long-lived neutron star. *Phys. Rev.* D **95** (6), 063016. arXiv:1701.08738.

CIOLFI, R., KASTAUN, W., KALINANI, J. V. & GIACOMAZZO, B. 2019 First 100 ms of a long-lived magnetized neutron star formed in a binary neutron star merger. *Phys. Rev.* D **100** (2), 023005. arXiv:1904.10222.

CIOLFI, R. & REZZOLLA, L. 2013 Twisted-torus configurations with large toroidal magnetic fields in relativistic stars. *MNRAS* **435**, L43–L47. arXiv:1306.2803.

COHEN, E., KATZ, J. I., PIRAN, T., SARI, R., PREECE, R. D. & BAND, D. L. 1997 Possible evidence for relativistic shocks in gamma-ray bursts. *Astrophys. J.* **488** (1), 330–337. arXiv:astro-ph/9703120.

COMISSO, L., LINGAM, M., HUANG, Y. M. & BHATTACHARJEE, A. 2016 General theory of the plasmoid instability. *Phys. Plasmas* **23** (10), 100702. arXiv:1608.04692.

COULTER, D. A., FOLEY, R. J., KILPATRICK, C. D., DROUT, M. R., PIRO, A. L., SHAPPEE, B. J., SIEBERT, M. R., SIMON, J. D., ULLOA, N., KASEN, D., *et al.* 2017 Swope supernova survey 2017a (SSS17a), the optical counterpart to a gravitational wave source. *Science* **358**, 1556–1558. arXiv:1710.05452.

CRIDER, A., LIANG, E. P., SMITH, I. A., PREECE, R. D., BRIGGS, M. S., PENDLETON, G. N., PACIESAS, W. S., BAND , D. L. & MATTESON, J. L. 1997 Evolution of the low-energy photon spectral in gamma-ray bursts. *Astrophys. J. Lett.* **479** (1), L39–L42. arXiv:astro-ph/9612118.

CRINQUAND, B., CERUTTI, B. & DUBUS, G. 2019 Kinetic modeling of the electromagnetic precursor from an axisymmetric binary pulsar coalescence. *A&A* **622**, A161. arXiv:1812.05898.

CUTLER, C. 2002 Gravitational waves from neutron stars with large toroidal B fields. *Phys. Rev.* D **66** (8), 084025. arXiv:gr-qc/0206051.

DAI, Z. G. & LU, T. 1998 γ-ray bursts and afterglows from rotating strange stars and neutron stars. *Phys. Rev. Lett.* **81** (20), 4301–4304. arXiv:astro-ph/9810332.

DAI, Z. G., WANG, X. Y., WU, X. F. & ZHANG, B. 2006 X-ray flares from postmerger millisecond pulsars. *Science* **311** (5764), 1127–1129. arXiv:astro-ph/0602525.

DAIGNE, F., BOŠNJAK, Ž. & DUBUS, G. 2011 Reconciling observed gamma-ray burst prompt spectra with synchrotron radiation? *A&A* **526**, A110. arXiv:1009.2636.

DAIGNE, F. & MOCHKOVITCH, R. 1998 Gamma-ray bursts from internal shocks in a relativistic wind: temporal and spectral properties. *MNRAS* **296** (2), 275–286. arXiv:astro-ph/9801245.

DAIGNE, F. & MOCHKOVITCH, R. 2002 The expected thermal precursors of gamma-ray bursts in the internal shock model. *MNRAS* **336** (4), 1271–1280. arXiv:astro-ph/0207456.

DAINOTTI, M. G., CARDONE, V. F. & CAPOZZIELLO, S. 2008 A time-luminosity correlation for γ-ray bursts in the X-rays. *MNRAS* **391** (1), L79–L83. arXiv:0809.1389.

DALL'OSSO, S., PERNA, R., TANAKA, T. L. & MARGUTTI, R. 2017 Flares in gamma-ray bursts: disc fragmentation and evolution. *MNRAS* **464** (4), 4399–4407. arXiv:1610.05302.

DALL'OSSO, S., SHORE, S. N. & STELLA, L. 2009 Early evolution of newly born magnetars with a strong toroidal field. *MNRAS* **398** (4), 1869–1885. arXiv:0811.4311.

DALL'OSSO, S., STELLA, L. & PALOMBA, C. 2018 Neutron star bulk viscosity, 'spin-flip' and GW emission of newly born magnetars. *MNRAS* **480** (1), 1353–1362. arXiv:1806.11164.

DALL'OSSO, S., STRATTA, G., GUETTA, D., COVINO, S., DE CESARE, G. & STELLA, L. 2011 Gamma-ray bursts afterglows with energy injection from a spinning down neutron star. *A&A* **526**, A121. arXiv:1004.2788.

D'AVANZO, P., CAMPANA, S., SALAFIA, O. S., GHIRLANDA, G., GHISELLINI, G., MELANDRI, A., BERNARDINI, M. G., BRANCHESI, M., CHASSANDE-MOTTIN, E., COVINO, S., *et al.* 2018 The evolution of the X-ray afterglow emission of GW 170817/ GRB 170817A in XMM-Newton observations. *A&A* **613**, L1. arXiv:1801.06164.

D'AVANZO, P., SALVATERRA, R., BERNARDINI, M. G., NAVA, L., CAMPANA, S., COVINO, S., D'ELIA, V., GHIRLANDA, G., GHISELLINI, G., MELANDRI, A., *et al.* 2014 A complete sample of bright swift short gamma-ray bursts. *MNRAS* **442** (3), 2342–2356. arXiv:1405.5131.

DAVIES, M. B., BENZ, W., PIRAN, T. & THIELEMANN, F. K. 1994 Merging neutron stars. I. Initial results for coalescence of noncorotating systems. *Astrophys. J.* **431**, 742. arXiv:astro-ph/9401032.

DERISHEV, E. V., KOCHAROVSKY, V. V. & KOCHAROVSKY, V. V. 2001 Physical parameters and emission mechanism in gamma-ray bursts. *A&A* **372**, 1071–1077. arXiv:astro-ph/0006239.

DESSART, L., OTT, C. D., BURROWS, A., ROSSWOG, S. & LIVNE, E. 2009 Neutrino signatures and the neutrino-driven wind in binary neutron star mergers. *Astrophys. J.* **690**, 1681–1705. arXiv:0806.4380.

DRENKHAHN, G. 2002 Acceleration of GRB outflows by Poynting flux dissipation. *A&A* **387**, 714–724. arXiv:astro-ph/0112509.

DRENKHAHN, G. & SPRUIT, H. C. 2002 Efficient acceleration and radiation in Poynting flux powered GRB outflows. *A&A* **391**, 1141–1153. arXiv:astro-ph/0202387.

DROUT, M. R., PIRO, A. L., SHAPPEE, B. J., KILPATRICK, C. D., SIMON, J. D., CONTRERAS, C., COULTER, D. A., FOLEY, R. J., SIEBERT, M. R., MORRELL, N., *et al.* 2017 Light curves of the neutron star merger GW170817/SSS17a: implications for r-process nucleosynthesis. *Science* **358**, 1570–1574. arXiv:1710.05443.

DUEZ, M. D., LIU, Y. T., SHAPIRO, S. L., SHIBATA, M. & STEPHENS, B. C. 2006 Collapse of magnetized hypermassive neutron stars in general relativity. *Phys. Rev. Lett.* **96** (3), 031101. arXiv:astro-ph/0510653.

EICHLER, D., LIVIO, M., PIRAN, T. & SCHRAMM, D. N. 1989 Nucleosynthesis, neutrino bursts and gamma-rays from coalescing neutron stars. *Nature* **340**, 126–128.

EVANS, P. A., BEARDMORE, A. P., PAGE, K. L., OSBORNE, J. P., O'BRIEN, P. T., WILLINGALE, R., STARLING, R. L. C., BURROWS, D. N., GODET, O., VETERE, L., *et al.* 2009 Methods and results of an automatic analysis of a complete sample of Swift-XRT observations of GRBs. *MNRAS* **397** (3), 1177–1201. arXiv:0812.3662.

FALCONE, A. D., MORRIS, D., RACUSIN, J., CHINCARINI, G., MORETTI, A., ROMANO, P., BURROWS, D. N., PAGANI, C., STROH, M., GRUPE, D., *et al.* 2007 The first survey of X-ray flares from gamma-ray bursts observed by swift: spectral properties and energetics. *Astrophys. J.* **671** (2), 1921–1938. arXiv:0706.1564.

FENIMORE, E. E., MADRAS, C. D. & NAYAKSHIN, S. 1996 Expanding relativistic shells and gamma-ray burst temporal structure. *Astrophys. J.* **473**, 998. arXiv:astro-ph/9607163.

FERMI, E. 1949 On the origin of the cosmic radiation. *Phys. Rev.* **75**, 1169–1174.

FERNÁNDEZ, R., QUATAERT, E., SCHWAB, J., KASEN, D. & ROSSWOG, S. 2015 The interplay of disc wind and dynamical ejecta in the aftermath of neutron star-black hole mergers. *MNRAS* **449** (1), 390–402. arXiv:1412.5588.

FERNÁNDEZ, R., TCHEKHOVSKOY, A., QUATAERT, E., FOUCART, F. & KASEN, D. 2019 Long-term GRMHD simulations of neutron star merger accretion discs: implications for electromagnetic counterparts. *Mon. Not. R. Astron. Soc.* **482** (3), 3373–3393. arXiv:1808.00461.

FISHBACH, M., GRAY, R., MAGAÑA HERNANDEZ, I., QI, H., SUR, A., ACERNESE, F., AIELLO, L., ALLOCCA, A., ALOY, M. A., AMATO, A., *et al.* 2019 A standard siren measurement of the hubble constant from GW170817 without the electromagnetic counterpart. *Astrophys. J. Lett.* **871** (1), L13. arXiv:1807.05667.

FONG, W., BERGER, E., CHORNOCK, R., MARGUTTI, R., LEVAN, A. J., TANVIR, N. R., TUNNICLIFFE, R. L., CZEKALA, I., FOX, D. B., PERLEY, D. A., *et al.* 2013 Demographics of the galaxies hosting short-duration gamma-ray bursts. *Astrophys. J.* **769** (1), 56. arXiv:1302.3221.

FONG, W., BERGER, E., FOX, D. B., 2010, Hubble Space Telescope Observations of Short Gamma-Ray Burst Host Galaxies: Morphologies, Offsets, and Local Environments, *Astrophys. J.* **708** (1), 9–25.

FOUCART, F., DEATON, M. B., DUEZ, M. D., O'CONNOR, E., OTT, C. D., HAAS, R., KIDDER, L. E., PFEIFFER, H. P., SCHEEL, M. A. & SZILAGYI, B. 2014 Neutron star-black hole mergers with a nuclear equation of state and neutrino cooling: dependence in the binary parameters. *Phys. Rev.* D **90** (2), 024026. arXiv:1405.1121.

FRAIL, D. A., KULKARNI, S. R., SARI, R., DJORGOVSKI, S. G., BLOOM, J. S., GALAMA, T. J., REICHART, D. E., BERGER, E., HARRISON, F. A., PRICE, P. A., *et al.* 2001 Beaming in gamma-ray bursts: evidence for a standard energy reservoir. *Astrophys. J. Lett.* **562** (1), L55–L58. arXiv:astro-ph/0102282.

FRONTERA, F., AMATI, L., COSTA, E., MULLER, J. M., PIAN, E., PIRO, L., SOFFITTA, P., TAVANI, M., CASTRO-TIRADO, A., DAL FIUME, D., *et al.* 2000 Prompt and delayed emission properties of gamma-ray bursts observed with BeppoSAX. *Astrophys. J. Suppl.* **127** (1), 59–78. arXiv:astro-ph/9911228.

FRUCHTER, A. S., LEVAN, A. J., STROLGER, L., VREESWIJK, P. M., THORSETT, S. E., BERSIER, D., BURUD, I., CASTRO CERÓN, J. M., CASTRO-TIRADO, A. J., CONSELICE, C., *et al.* 2006 Long γ-ray bursts and core-collapse supernovae have different environments. *Nature* **441** (7092), 463–468. arXiv:astro-ph/0603537.

FUJIBAYASHI, S., KIUCHI, K., NISHIMURA, N., SEKIGUCHI, Y. & SHIBATA, M. 2018 Mass ejection from the remnant of a binary neutron star merger: viscous-radiation hydrodynamics study. *Astrophys. J.* **860** (1), 64. arXiv:1711.02093.

GAENSLER, B. M. & SLANE, P. O. 2006 The evolution and structure of pulsar wind nebulae. *ARA&A* **44** (1), 17–47. arXiv:astro-ph/0601081.

GAO, H., DING, X., WU, X.-F., DAI, Z.-G. & ZHANG, B. 2015 GRB 080503 late afterglow re-brightening: signature of a magnetar-powered merger-nova. *Astrophys. J.* **807**, 163. arXiv:1506.06816.

GENG, J.-J., HUANG, Y.-F., WU, X.-F., ZHANG, B. & ZONG, H.-S. 2018 Low-energy spectra of gamma-ray bursts from cooling electrons. *Astrophys. J. Suppl.* **234** (1), 3. arXiv:1709.05899.

GHIRLANDA, G., CELOTTI, A. & GHISELLINI, G. 2002 Time resolved spectral analysis of bright gamma ray bursts. *A&A* **393**, 409–423. arXiv:astro-ph/0206377.

GHIRLANDA, G., SALAFIA, O. S., PARAGI, Z., GIROLETTI, M., YANG, J., MARCOTE, B., BLANCHARD, J., AGUDO, I., AN, T., BERNARDINI, M. G., *et al.* 2019 Compact radio emission indicates a structured jet was produced by a binary neutron star merger. *Science* **363** (6430), 968–971. arXiv:1808.00469.

GHISELLINI, G. 2013 *Radiative Processes in High Energy Astrophysics*. Lecture Notes in Physics. vol. 873. Springer International Publishing Switzerland.

GHISELLINI, G., CELOTTI, A. & LAZZATI, D. 2000 Constraints on the emission mechanisms of gamma-ray bursts. *MNRAS* **313** (1), L1–L5. arXiv:astro-ph/9912461.

GHISELLINI, G., GHIRLANDA, G., OGANESYAN, G., ASCENZI, S., NAVA, L., CELOTTI, A., SALAFIA, O. S., RAVASIO, M. E. & RONCHI, M. 2020 Proton-synchrotron as the radiation mechanism of the prompt emission of gamma-ray bursts? *A&A* **636**, A82. arXiv:1912.02185.

GIACOMAZZO, B. & PERNA, R. 2013 Formation of stable magnetars from binary neutron star mergers. *Astrophys. J. Lett.* **771**, L26. arXiv:1306.1608.

GIACOMAZZO, B., ZRAKE, J., DUFFELL, P. C., MACFADYEN, A. I. & PERNA, R. 2015 Producing magnetar magnetic fields in the merger of binary neutron stars. *Astrophys. J.* **809**, 39. arXiv:1410.0013.

GIANNIOS, D. 2006 Prompt emission spectra from the photosphere of a GRB. *A&A* **457** (3), 763–770. arXiv:astro-ph/0602397.

GILL, R., GRANOT, J. & BENIAMINI, P. 2020 GRB spectrum from gradual dissipation in a magnetized outflow. *MNRAS* **499** (1), 1356–1372. arXiv:2008.10729.

GILMOZZI, R. & SPYROMILIO, J. 2007 The European extremely large telescope (E-ELT). *The Messenger* **127**, 11.

GOLDREICH, P. & JULIAN, W. H. 1970 Stellar winds. *Astrophys. J.* **160**, 971.

GOLDSTEIN, A., VERES, P., BURNS, E., BRIGGS, M. S., HAMBURG, R., KOCEVSKI, D., WILSON-HODGE, C. A., PREECE, R. D., POOLAKKIL, S., ROBERTS, O. J., *et al.* 2017 An ordinary short gamma-ray burst with extraordinary implications: fermi-GBM detection of GRB 170817a. *Astrophys. J. Lett.* **848** (2), L14.

GOODMAN, J. 1986 Are gamma-ray bursts optically thick? *Astrophys. J. Lett.* **308**, L47.

GOODMAN, J., DAR, A. & NUSSINOV, S. 1987 Neutrino annihilation in type II supernovae. *Astrophys. J. Lett.* **314**, L7.

GRANOT, J., KOMISSAROV, S. S. & SPITKOVSKY, A. 2011 Impulsive acceleration of strongly magnetized relativistic flows. *MNRAS* **411** (2), 1323–1353. arXiv:1004.0959.

HAGGARD, D., NYNKA, M., RUAN, J. J., KALOGERA, V., CENKO, S. B., EVANS, P. & KENNEA, J. A. 2017 A deep chandra X-ray study of neutron star coalescence GW170817. *Astrophys. J. Lett.* **848**, L25. arXiv:1710.05852.

HAJELA, A., MARGUTTI, R., KATHIRGAMARAJU, A., GIANNIOS, D., LASKAR, T., ALEXANDER, K. D., COPPEJANS, D. L., FONG, W. & BERGER, E. 2020 X-ray emission from GW170817 ∼2.5 years after the merger. *Res. Notes Am. Astron. Soc.* **4** (5), 68.

HANSEN, B. M. S. & LYUTIKOV, M. 2001 Radio and X-ray signatures of merging neutron stars. *MNRAS* **322** (4), 695–701. arXiv:astro-ph/0003218.

HEAVENS, A. F. & DRURY, L. O'C. 1988 Relativistic shocks and particle acceleration. *MNRAS* **235**, 997–1009.

HOTOKEZAKA, K., KYUTOKU, K., OKAWA, H., SHIBATA, M. & KIUCHI, K. 2011 Binary neutron star mergers: dependence on the nuclear equation of state. *Phys. Rev.* D **83** (12), 124008. arXiv:1105.4370.

IVEZIĆ, Ž., KAHN, S. M., TYSON, J. A., ABEL, B., ACOSTA, E., ALLSMAN, R., ALONSO, D., ALSAYYAD, Y., ANDERSON, S. F., ANDREW, J., *et al.* 2019 LSST: from science drivers to reference design and anticipated data products. *Astrophys. J.* **873** (2), 111. arXiv:0805.2366.

JUST, O., OBERGAULINGER, M., JANKA, H.-T., BAUSWEIN, A. & SCHWARZ, N. 2016 Neutron-star merger ejecta as obstacles to neutrino-powered jets of gamma-ray bursts. *Astrophys. J. Lett.* **816**, L30. arXiv:1510.04288.

KANN, D. A., KLOSE, S., ZHANG, B., COVINO, S., BUTLER, N. R., MALESANI, D., NAKAR, E., WILSON, A. C., ANTONELLI, L. A., CHINCARINI, G., *et al.* 2011 The afterglows of swift-era gamma-ray bursts. II. Type I GRB versus type II GRB optical afterglows. *Astrophys. J.* **734** (2), 96. arXiv:0804.1959.

KAWAMURA, T., GIACOMAZZO, B., KASTAUN, W., CIOLFI, R., ENDRIZZI, A., BAIOTTI, L. & PERNA, R. 2016 Binary neutron star mergers and short gamma-ray bursts: effects of magnetic field orientation, equation of state, and mass ratio. *Phys. Rev.* D **94**, 064012.

KIUCHI, K., CERDÁ-DURÁN, P., KYUTOKU, K., SEKIGUCHI, Y. & SHIBATA, M. 2015 Efficient magnetic-field amplification due to the Kelvin–Helmholtz instability in binary neutron star mergers. *Phys. Rev.* D **92** (12), 124034. arXiv:1509.09205.

KIUCHI, K., KYUTOKU, K., SEKIGUCHI, Y., SHIBATA, M. & WADA, T. 2014 High resolution numerical relativity simulations for the merger of binary magnetized neutron stars. *Phys. Rev.* D **90** (4), 041502. arXiv:1407.2660.

KOBAYASHI, S., PIRAN, T. & SARI, R. 1997 Can internal shocks produce the variability in gamma-ray bursts? *Astrophys. J.* **490**, 92. arXiv:astro-ph/9705013.

KOMISSAROV, S. S. 2004 Electrodynamics of black hole magnetospheres. *MNRAS* **350** (2), 427–448.

KOUVELIOTOU, C., MEEGAN, C. A., FISHMAN, G. J., BHAT, N. P., BRIGGS, M. S., KOSHUT, T. M., PACIESAS, W. S. & PENDLETON, G. N. 1993 Identification of two classes of gamma-ray bursts. *Astrophys. J. Lett.* **413**, L101–L104.

KULKARNI, S. R. 2005 Modeling supernova-like explosions associated with gamma-ray bursts with short durations. arXiv:astro-ph/0510256.

KUMAR, P. & MCMAHON, E. 2008 A general scheme for modelling γ-ray burst prompt emission. *MNRAS* **384** (1), 33–63. arXiv:0802.2704.

KUMAR, P., NARAYAN, R. & JOHNSON, J. L. 2008 Properties of gamma-ray burst progenitor stars. *Science* **321** (5887), 376. arXiv:0807.0445.

KUMAR, P. & PANAITESCU, A. 2000 Afterglow emission from naked gamma-ray bursts. *Astrophys. J. Lett.* **541** (2), L51–L54. arXiv:astro-ph/0006317.

KUMAR, P. & PIRAN, T. 2000 Energetics and luminosity function of gamma-ray bursts. *Astrophys. J.* **535** (1), 152–157. arXiv:astro-ph/9909014.

KUMAR, P. & ZHANG, B. 2015 The physics of gamma-ray bursts relativistic jets. *PhR* **561**, 1–109. arXiv:1410.0679.

LAI, D. 2012 DC circuit powered by orbital motion: magnetic interactions in compact object binaries and exoplanetary systems. *Astrophys. J. Lett.* **757**, L3. arXiv:1206.3723.

LANDER, S. K. & JONES, D. I. 2020 Magnetar birth: rotation rates and gravitational-wave emission. *MNRAS*. arXiv:1910.14336.

LATTIMER, J. M. & SCHRAMM, D. N. 1974 Black-hole-neutron-star collisions. *Astrophys. J. Lett.* **192**, L145.

LAZZATI, D., MORSONY, B. J., MARGUTTI, R. & BEGELMAN, M. C. 2013 Photospheric emission as the dominant radiation mechanism in long-duration gamma-ray bursts. *Astrophys. J.* **765** (2), 103. arXiv:1301.3920.

LAZZATI, D. & PERNA, R. 2019 Jet-cocoon outflows from neutron star mergers: structure, light curves, and fundamental physics. *Astrophys. J.* **881** (2), 89. arXiv:1904.08425.

LEE, W. H., RAMIREZ-RUIZ, E. & LÓPEZ-CÁMARA, D. 2009 Phase transitions and He-synthesis-driven winds in neutrino cooled accretion disks: prospects for late flares in short gamma-ray bursts. *Astrophys. J. Lett.* **699**, L93–L96. arXiv:0904.3752.

LEVINSON, A. & NAKAR, E. 2020 Physics of radiation mediated shocks and its applications to GRBs, supernovae, and neutron star mergers. *PhR* **866**, 1–46. arXiv:1909.10288.

LI, L.-X. & PACZYŃSKI, B. 1998 Transient events from neutron star mergers. *Astrophys. J. Lett.* **507**, L59–L62. arXiv:astro-ph/9807272.

LIANG, E., KUSUNOSE, M., SMITH, I. A. & CRIDER, A. 1997 Physical model of gamma-ray burst spectral evolution. *Astrophys. J. Lett.* **479** (1), L35–L38.

LIU, T., GU, W.-M. & ZHANG, B. 2017 Neutrino-dominated accretion flows as the central engine of gamma-ray bursts. *New Astron. Rev.* **79**, 1–25. arXiv:1705.05516.

LLOYD, N. M. & PETROSIAN, V. 2000 Synchrotron radiation as the source of gamma-ray burst spectra. *Astrophys. J.* **543** (2), 722–732. arXiv:astro-ph/0007061.

LOUREIRO, N. F., SAMTANEY, R., SCHEKOCHIHIN, A. A. & UZDENSKY, D. A. 2012 Magnetic reconnection and stochastic plasmoid chains in high-Lundquist-number plasmas. *Phys. Plasmas* **19** (4), 042303–042303. arXiv:1108.4040.

LYONS, N., O'BRIEN, P. T., ZHANG, B., WILLINGALE, R., TROJA, E. & STARLING, R. L. C. 2010 Can X-ray emission powered by a spinning-down magnetar explain some gamma-ray burst light-curve features? *MNRAS* **402** (2), 705–712. arXiv:0908.3798.

MAGIC COLLABORATION, ACCIARI, V. A., ANSOLDI, S., ANTONELLI, L. A., ARBET ENGELS, A., BAACK, D., BABIĆ, A., BANERJEE, B., BARRES DE ALMEIDA, U., BARRIO, J. A., BECERRA GONZÁLEZ, J., *et al.* 2019 Teraelectronvolt emission from the γ-ray burst GRB 190114C. *Nature* **575** (7783), 455–458. arXiv:2006.07249.

MARGALIT, B., METZGER, B. D. & BELOBORODOV, A. M. 2015 Does the collapse of a supramassive neutron star leave a debris disk? *Phys. Rev. Lett.* **115** (17), 171101. arXiv:1505.01842.

MARGUTTI, R., ZANINONI, E., BERNARDINI, M. G., CHINCARINI, G., PASOTTI, F., GUIDORZI, C., ANGELINI, L., BURROWS, D. N., CAPALBI, M., EVANS, P. A., *et al.* 2013 The prompt-afterglow connection in gamma-ray bursts: a comprehensive statistical analysis of Swift X-ray light curves. *MNRAS* **428** (1), 729–742. arXiv:1203.1059.

MARTIN, D., PEREGO, A., ARCONES, A., THIELEMANN, F. K., KOROBKIN, O. & ROSSWOG, S. 2015 Neutrino-driven winds in the aftermath of a neutron star merger: nucleosynthesis and electromagnetic transients. *Astrophys. J.* **813** (1), 2. arXiv:1506.05048.

MCWILLIAMS, S. T. & LEVIN, J. 2011 Electromagnetic extraction of energy from black-hole-neutron-star binaries. *Astrophys. J.* **742**, 90. arXiv:1101.1969.

MEDVEDEV, M. V. 2000 Theory of 'Jitter' radiation from small-scale random magnetic fields and prompt emission from gamma-ray burst shocks. *Astrophys. J.* **540** (2), 704–714. arXiv:astro-ph/0001314.

MELANDRI, A., COVINO, S., ROGANTINI, D., SALVATERRA, R., SBARUFATTI, B., BERNARDINI, M. G., CAMPANA, S., D'AVANZO, P., D'ELIA, V., FUGAZZA, D., *et al.* 2014 Optical and X-ray rest-frame light curves of the BAT6 sample. *A&A* **565**, A72. arXiv:1403.3245.

MEREGHETTI, S., PONS, J. A. & MELATOS, A. 2015 Magnetars: properties, origin and evolution. *Space Sci. Rev.* **191** (1–4), 315–338. arXiv:1503.06313.

MERLONI, A., PREDEHL, P., BECKER, W., BÖHRINGER, H., BOLLER, T., BRUNNER, H., BRUSA, M., DENNERL, K., FREYBERG, M., FRIEDRICH, P., *et al.* 2012 eROSITA science book: mapping the structure of the energetic universe. e-prints. arXiv:1209.3114.

MESZAROS, P. & REES, M. J. 1993 Gamma-ray bursts: multiwaveband spectral predictions for blast wave models. *Astrophys. J. Lett.* **418**, L59. arXiv:astro-ph/9309011.

MÉSZÁROS, P. & REES, M. J. 1997*a* Optical and long-wavelength afterglow from gamma-ray bursts. *Astrophys. J.* **476** (1), 232–237. arXiv:astro-ph/9606043.

MÉSZÁROS, P. & REES, M. J. 1997*b* Optical and long-wavelength afterglow from gamma-ray bursts. *Astrophys. J.* **476** (1), 232–237. arXiv:astro-ph/9606043.

MESZAROS, P., REES, M. J. & PAPATHANASSIOU, H. 1994 Spectral properties of blast-wave models of gamma-ray burst sources. *Astrophys. J.* **432**, 181. arXiv:astro-ph/9311071.

METZGER, B. D. 2017 Kilonovae. *Living Rev. Relativ.* **20** (1), 3.

METZGER, B. D., GIANNIOS, D., THOMPSON, T. A., BUCCIANTINI, N. & QUATAERT, E. 2011 The protomagnetar model for gamma-ray bursts. *MNRAS* **413** (3), 2031–2056. arXiv:1012.0001.

METZGER, B. D., MARTÍNEZ-PINEDO, G., DARBHA, S., QUATAERT, E., ARCONES, A., KASEN, D., THOMAS, R., NUGENT, P., PANOV, I. V. & ZINNER, N. T. 2010 Electromagnetic counterparts of compact object mergers powered by the radioactive decay of r-process nuclei. *Mon. Not. R. Astron. Soc.* **406** (4), 2650.

METZGER, B. D. & PIRO, A. L. 2014 Optical and X-ray emission from stable millisecond magnetars formed from the merger of binary neutron stars. *MNRAS* **439**, 3916–3930. arXiv:1311.1519.

MIRABEL, I. F. & RODRÍGUEZ, L. F. 1999 Sources of relativistic jets in the galaxy. *ARA&A* **37**, 409–443. arXiv:astro-ph/9902062.

MOOLEY, K. P., DELLER, A. T., GOTTLIEB, O., NAKAR, E., HALLINAN, G., BOURKE, S., FRAIL, D. A., HORESH, A., CORSI, A. & HOTOKEZAKA, K. 2018 Superluminal motion of a relativistic jet in the neutron star merger GW170817. e-prints. arXiv:1806.09693.

MOST, E. R. & PHILIPPOV, A. A. 2020 Electromagnetic precursors to gravitational-wave events: numerical simulations of flaring in pre-merger binary neutron star magnetospheres. *Astrophys. J. Lett.* **893** (1), L6. arXiv:2001.06037.

MÖSTA, P., RADICE, D., HAAS, R., SCHNETTER, E. & BERNUZZI, S. 2020 A magnetar engine for short GRBs and Kilonovae. *Astrophys. J. Lett.* **901** (2), L37. arXiv:2003.06043.

NAKAR, E. 2007 Short-hard gamma-ray bursts. *PhR* **442** (1–6), 166–236. arXiv:astro-ph/0701748.

NAKAR, E. 2019 The electromagnetic counterparts of compact binary mergers. e-prints. arXiv:1912.05659.

NAKAR, E. & PIRAN, T. 2011 Detectable radio flares following gravitational waves from mergers of binary neutron stars. *Nature* **478** (7367), 82–84. arXiv:1102.1020.

NARAYAN, R. & KUMAR, P. 2009 A turbulent model of gamma-ray burst variability. *MNRAS* **394** (1), L117–L120. arXiv:0812.0018.

NOUSEK, J. A., KOUVELIOTOU, C., GRUPE, D., PAGE, K. L., GRANOT, J., RAMIREZ-RUIZ, E., PATEL, S. K., BURROWS, D. N., MANGANO, V., BARTHELMY, S., *et al.* 2006 Evidence for a canonical gamma-ray burst afterglow light curve in the swift XRT data. *Astrophys. J.* **642** (1), 389–400. arXiv:astro-ph/0508332.

O'BRIEN, P. T., WILLINGALE, R., OSBORNE, J., GOAD, M. R., PAGE, K. L., VAUGHAN, S., ROL, E., BEARDMORE, A., GODET, O., HURKETT, C. P., *et al.* 2006 The early X-ray emission from GRBs. *Astrophys. J.* **647** (2), 1213–1237. arXiv:astro-ph/0601125.

OGANESYAN, G., ASCENZI, S., BRANCHESI, M., SALAFIA, O. S., DALL'OSSO, S. & GHIRLANDA, G. 2020 Structured jets and X-ray plateaus in gamma-ray burst phenomena. *Astrophys. J.* **893** (2), 88. arXiv:1904.08786.

OGANESYAN, G., NAVA, L., GHIRLANDA, G. & CELOTTI, A. 2017 Detection of low-energy breaks in gamma-ray burst prompt emission spectra. *Astrophys. J.* **846** (2), 137. arXiv:1709.04689.

OGANESYAN, G., NAVA, L., GHIRLANDA, G., MELANDRI, A. & CELOTTI, A. 2019 Prompt optical emission as a signature of synchrotron radiation in gamma-ray bursts. *A&A* **628**, A59. arXiv:1904.11086.

PACINI, F. 1967 Energy emission from a neutron star. *Nature* **216** (5115), 567–568.

PACZYNSKI, B. 1986 Gamma-ray bursters at cosmological distances. *Astrophys. J. Lett.* **308**, L43–L46.

PACZYNSKI, B. & RHOADS, J. E. 1993 Radio transients from gamma-ray bursters. *Astrophys. J. Lett.* **418**, L5. arXiv:astro-ph/9307024.

PALENZUELA, C., LEHNER, L., PONCE, M., LIEBLING, S. L., ANDERSON, M., NEILSEN, D. & MOTL, P. 2013 Electromagnetic and gravitational outputs from binary-neutron-star coalescence. *Phys. Rev. Lett.* **111** (6), 061105. arXiv:1301.7074.

PANAITESCU, A. 2019 Adiabatic and radiative cooling of relativistic electrons applied to synchrotron spectra and light curves of gamma-ray burst pulses. *Astrophys. J.* **886** (2), 106. arXiv:1905.10440.

PANAITESCU, A. & KUMAR, P. 2001 Jet energy and other parameters for the afterglows of GRB 980703, GRB 990123, GRB 990510, and GRB 991216 determined from modeling of multifrequency data. *Astrophys. J.* **554** (2), 667–677. arXiv:astro-ph/0010257.

PANAITESCU, A., KUMAR, P. & NARAYAN, R. 2001 Observational prospects for afterglows of short-duration gamma-ray bursts. *Astrophys. J. Lett.* **561** (2), L171–L174. arXiv:astro-ph/0108132.

PANAITESCU, A., VESTRAND, W. T. & WOŹNIAK, P. 2013 An external-shock model for gamma-ray burst afterglow 130427A. *MNRAS* **436** (4), 3106–3111. arXiv:1311.5867.

PASCHALIDIS, V., RUIZ, M. & SHAPIRO, S. L. 2015 Relativistic simulations of black hole-neutron star coalescence: the jet emerges. *Astrophys. J. Lett.* **806**, L14. arXiv:1410.7392.

PE'ER, A. 2008 Temporal evolution of thermal emission from relativistically expanding plasma. *Astrophys. J.* **682** (1), 463–473. arXiv:0802.0725.

PEREGO, A., RADICE, D. & BERNUZZI, S. 2017*a* AT 2017gfo: an anisotropic and three-component Kilonova counterpart of GW170817. *Astrophys. J. Lett.* **850** (2), L37. arXiv:1711.03982.

PEREGO, A., ROSSWOG, S., CABEZÓN, R. M., KOROBKIN, O., KÄPPELI, R., ARCONES, A. & LIEBENDÖRFER, M. 2014 Neutrino-driven winds from neutron star merger remnants. *MNRAS* **443**, 3134–3156. arXiv:1405.6730.

PEREGO, A., YASIN, H. & ARCONES, A. 2017*b* Neutrino pair annihilation above merger remnants: implications of a long-lived massive neutron star. *J. Phys.* G *Nucl. Phys.* **44** (8), 084007. arXiv:1701.02017.

PERNA, R., ARMITAGE, P. J. & ZHANG, B. 2006 Flares in long and short gamma-ray bursts: a common origin in a hyperaccreting accretion disk. *Astrophys. J. Lett.* **636**, L29–L32. arXiv:astro-ph/0511506.

PETROPOULOU, M., DIMITRAKOUDIS, S., MASTICHIADIS, A. & GIANNIOS, D. 2014 Hadronic supercriticality as a trigger for γ-ray burst emission. *MNRAS* **444** (3), 2186–2199. arXiv:1407.2915.

PETROPOULOU, M., SIRONI, L., SPITKOVSKY, A. & GIANNIOS, D. 2019 Relativistic magnetic reconnection in electron-positron-proton plasmas: implications for jets of active galactic nuclei. *Astrophys. J.* **880** (1), 37. arXiv:1906.03297.

PIAN, E., D'AVANZO, P., BENETTI, S., BRANCHESI, M., BROCATO, E., CAMPANA, S., CAPPELLARO, E., COVINO, S., D'ELIA, V., FYNBO, J. P. U., *et al.* 2017 Spectroscopic identification of r-process nucleosynthesis in a double neutron-star merger. *Nature* **551**, 67–70. arXiv:1710.05858.

PIRAN, T. 1995 In *Some Unsolved Problems in Astrophysics* (eds. J. Bahcall & J. Ostriker), p. 273.

PIRAN, T. 1999 Gamma-ray bursts and the fireball model. *PhR* **314** (6), 575–667. arXiv:astro-ph/9810256.

PIRAN, T. 2004 The physics of gamma-ray bursts. *Rev. Mod. Phys.* **76**, 1143–1210. arXiv:astro-ph/0405503.

PIRO, A. L. 2012 Magnetic interactions in coalescing neutron star binaries. *Astrophys. J.* **755** (1), 80. arXiv:1205.6482.

PREECE, R. D., BRIGGS, M. S., MALLOZZI, R. S., PENDLETON, G. N., PACIESAS, W. S. & BAND, D. L. 1998 The synchrotron shock model confronts a 'Line of Death' in the BATSE gamma-ray burst data. *Astrophys. J. Lett.* **506** (1), L23–L26. arXiv:astro-ph/9808184.

PRICE, D. J. & ROSSWOG, S. 2006 Producing ultrastrong magnetic fields in neutron star mergers. *Science* **312**, 719–722. arXiv:astro-ph/0603845.

PROGA, D. & ZHANG, B. 2006 The late time evolution of gamma-ray bursts: ending hyperaccretion and producing flares. *MNRAS* **370**, L61–L65. arXiv:astro-ph/0601272.

RADICE, D., PEREGO, A., HOTOKEZAKA, K., BERNUZZI, S., FROMM, S. A. & ROBERTS, L. F. 2018 Viscous-dynamical ejecta from binary neutron star mergers. *Astrophys. J. Lett.* **869** (2), L35. arXiv:1809.11163.

RAVASIO, M. E., GHIRLANDA, G., NAVA, L. & GHISELLINI, G. 2019 Evidence of two spectral breaks in the prompt emission of gamma-ray bursts. *A&A* **625**, A60. arXiv:1903.02555.

REES, M. J. & MESZAROS, P. 1994 Unsteady outflow models for cosmological gamma-ray bursts. *Astrophys. J. Lett.* **430**, L93–L96. arXiv:astro-ph/9404038.

REES, M. J. & MÉSZÁROS, P. 1998 Refreshed shocks and afterglow longevity in gamma-ray bursts. *Astrophys. J. Lett.* **496** (1), L1–L4. arXiv:astro-ph/9712252.

REES, M. J. & MÉSZÁROS, P. 2005 Dissipative photosphere models of gamma-ray bursts and X-ray flashes. *Astrophys. J.* **628** (2), 847–852. arXiv:astro-ph/0412702.

REZZOLLA, L., BAIOTTI, L., GIACOMAZZO, B., LINK, D. & FONT, J. A. 2010 Accurate evolutions of unequal-mass neutron-star binaries: properties of the torus and short GRB engines. *Class. Quant. Grav.* **27** (11), 114105. arXiv:1001.3074.

REZZOLLA, L., GIACOMAZZO, B., BAIOTTI, L., GRANOT, J., KOUVELIOTOU, C. & ALOY, M. A. 2011 The missing link: merging neutron stars naturally produce jet-like structures and can power short gamma-ray bursts. *Astrophys. J. Lett.* **732** (11), L6. arXiv:1101.4298.

RHOADS, J. E. 1997 How to tell a jet from a balloon: a proposed test for beaming in gamma-ray bursts. *Astrophys. J. Lett.* **487** (1), L1–L4. arXiv:astro-ph/9705163.

RHOADS, J. E. 1999 The dynamics and light curves of beamed gamma-ray burst afterglows. *Astrophys. J.* **525**, 737–749. arXiv:astro-ph/9903399.

ROSSWOG, S. 2005 Mergers of neutron star-black hole binaries with small mass ratios: nucleosynthesis, gamma-ray bursts, and electromagnetic transients. *Astrophys. J.* **634**, 1202–1213. arXiv:astro-ph/0508138.

ROSSWOG, S. 2015 The multi-messenger picture of compact binary mergers. *Intl J. Mod. Phys.* D **24**, 1530012–1530052. arXiv:1501.02081.

ROSSWOG, S., LIEBENDÖRFER, M., THIELEMANN, F.-K., DAVIES, M. B., BENZ, W. & PIRAN, T. 1999 Mass ejection in neutron star mergers. *A&A* **341**, 499–526. arXiv:astro-ph/9811367.

ROWLINSON, A., O'BRIEN, P. T., METZGER, B. D., TANVIR, N. R. & LEVAN, A. J. 2013 Signatures of magnetar central engines in short GRB light curves. *MNRAS* **430**, 1061–1087. arXiv:1301.0629.

RUDERMAN, M. 1975 Theories of gamma-ray bursts. In *Seventh Texas Symposium on Relativistic Astrophysics* (ed. P. G. Bergman, E. J. Fenyves & L. Motz), vol. 262, pp. 164–180. AAS, American Physical Society, and New York Academy of Sciences.

RUIZ, M., LANG, R. N., PASCHALIDIS, V. & SHAPIRO, S. L. 2016 Binary neutron star mergers: a jet engine for short gamma-ray bursts. *Astrophys. J. Lett.* **824**, L6. arXiv:1604.02455.

RYBICKI, G. B. & LIGHTMAN, A. P. 1986 *Radiative Processes in Astrophysics*. Wiley-VCH.

SALAFIA, O. S., BARBIERI, C., ASCENZI, S. & TOFFANO, M. 2019 Gamma-ray burst jet propagation, development of angular structure, and the luminosity function. e-prints. arXiv:1907.07599.

SALAFIA, O. S. & GIACOMAZZO, B. 2020 Accretion-to-jet energy conversion efficiency in GW170817. e-prints. arXiv:2006.07376.

SARI, R. & PIRAN, T. 1997 Variability in gamma-ray bursts: a clue. *Astrophys. J.* **485** (1), 270–273. arXiv:astro-ph/9701002.

SARI, R. & PIRAN, T. 1999 Predictions for the very early afterglow and the optical flash. *Astrophys. J.* **520** (2), 641–649. arXiv:astro-ph/9901338.

SARI, R., PIRAN, T. & HALPERN, J. P. 1999 Jets in gamma-ray bursts. *Astrophys. J. Lett.* **519**, L17–L20. arXiv:astro-ph/9903339.

SARI, R., PIRAN, T. & NARAYAN, R. 1998 Spectra and light curves of gamma-ray burst afterglows. *Astrophys. J. Lett.* **497** (1), L17–L20. arXiv:astro-ph/9712005.

SARIN, N., LASKY, P. D. & ASHTON, G. 2020 Gravitational waves or deconfined quarks: what causes the premature collapse of neutron stars born in short gamma-ray bursts? *Phys. Rev.* D **101** (6), 063021. arXiv:2001.06102.

SAVCHENKO, V., FERRIGNO, C., KUULKERS, E., BAZZANO, A., BOZZO, E., BRANDT, S., CHENEVEZ, J., COURVOISIER, T. J. -L., DIEHL, R., DOMINGO, A., *et al.* 2017 Integral detection

of the first prompt gamma-ray signal coincident with the gravitational-wave event gw170817. *Astrophys. J. Lett*. **848** (2), L15.

SHAPPEE, B. J., SIMON, J. D., DROUT, M. R., PIRO, A. L., MORRELL, N., PRIETO, J. L., KASEN, D., HOLOIEN, T. W. -S., KOLLMEIER, J. A., KELSON, D. D., *et al.* 2017 Early spectra of the gravitational wave source GW170817: evolution of a neutron star merger. *Science* **358**, 1574–1578. arXiv:1710.05432.

SHEMI, A. & PIRAN, T. 1990 The appearance of cosmic fireballs. *Astrophys. J. Lett*. **365**, L55.

SHIBATA, M. & TANIGUCHI, K. 2006 Merger of binary neutron stars to a black hole: disk mass, short gamma-ray bursts, and quasinormal mode ringing. *Phys. Rev.* D **73** (6), 064027. arXiv:astro-ph/0603145.

SHIBATA, M. & TANIGUCHI, K. 2011 Coalescence of black hole-neutron star binaries. *Living Rev. Relativ*. **14** (1), 6.

SHIBATA, M., TANIGUCHI, K. & URYU, K. 2005 Merger of binary neutron stars with realistic equations of state in full general relativity. *Phys. Rev.* D **71** (8), 084021. arXiv:gr-qc/0503119.

SIEGEL, D. M. & CIOLFI, R. 2016a Electromagnetic emission from long-lived binary neutron star merger remnants. I. Formulation of the problem. *Astrophys. J*. **819**, 14. arXiv:1508.07911.

SIEGEL, D. M. & CIOLFI, R. 2016b Electromagnetic emission from long-lived binary neutron star merger remnants. II. Lightcurves and spectra. *Astrophys. J*. **819**, 15. arXiv:1508.07939.

SIEGEL, D. M., CIOLFI, R., HARTE, A. I. & REZZOLLA, L. 2013 Magnetorotational instability in relativistic hypermassive neutron stars. *Phys. Rev.* D **87** (12), 121302. arXiv:1302.4368.

SIEGEL, D. M., CIOLFI, R. & REZZOLLA, L. 2014 Magnetically driven winds from differentially rotating neutron stars and X-ray afterglows of short gamma-ray bursts. *Astrophys. J. Lett*. **785**, L6. arXiv:1401.4544.

SIEGEL, D. M. & METZGER, B. D. 2017 Three-dimensional general-relativistic magnetohydrodynamic simulations of remnant accretion disks from neutron star mergers: outflows and r-process nucleosynthesis. *Phys. Rev. Lett*. **119** (23), 231102. arXiv:1705.05473.

SIEGEL, D. M. & METZGER, B. D. 2018 Three-dimensional GRMHD simulations of neutrino-cooled accretion disks from neutron star mergers. *Astrophys. J*. **858** (1), 52. arXiv:1711.00868.

SIRONI, L., KESHET, U. & LEMOINE, M. 2015a Relativistic shocks: particle acceleration and magnetization. *SSR* **191** (1–4), 519–544. arXiv:1506.02034.

SIRONI, L., PETROPOULOU, M. & GIANNIOS, D. 2015b Relativistic jets shine through shocks or magnetic reconnection? *MNRAS* **450** (1), 183–191. arXiv:1502.01021.

SIRONI, L. & SPITKOVSKY, A. 2011 Particle acceleration in relativistic magnetized collisionless electron-ion shocks. *Astrophys. J*. **726** (2), 75. arXiv:1009.0024.

SIRONI, L. & SPITKOVSKY, A. 2014 Relativistic reconnection: an efficient source of non-thermal particles. *Astrophys. J. Lett*. **783** (1), L21. arXiv:1401.5471.

SPRUIT, H. C., DAIGNE, F. & DRENKHAHN, G. 2001 Large scale magnetic fields and their dissipation in GRB fireballs. *A&A* **369**, 694–705. arXiv:astro-ph/0004274.

SRIDHAR, N., ZRAKE, J., METZGER, B. D., SIRONI, L. & GIANNIOS, D. 2020 Shock-powered radio precursors of neutron star mergers from accelerating relativistic binary winds. e-prints. arXiv:2010.09214.

STRATTA, G., CIOLFI, R., AMATI, L., BOZZO, E., GHIRLANDA, G., MAIORANO, E., NICASTRO, L., ROSSI, A., VINCIGUERRA, S., FRONTERA, F., *et al.* 2018 THESEUS: a key space mission concept for multi-messenger astrophysics. *Adv. Space Res*. **62** (3), 662–682. arXiv:1712.08153.

SYMBALISTY, E. & SCHRAMM, D. N. 1982 Neutron star collisions and the r-process. *Astrophys. Lett*. **22**, 143.

TAGLIAFERRI, G., GOAD, M., CHINCARINI, G., MORETTI, A., CAMPANA, S., BURROWS, D. N., PERRI, M., BARTHELMY, S. D., GEHRELS, N., KRIMM, H., *et al.* 2005 An unexpectedly rapid decline in the X-ray afterglow emission of long γ-ray bursts. *Nature* **436** (7053), 985–988. arXiv:astro-ph/0506355.

TANAKA, M. & HOTOKEZAKA, K. 2013 Radiative transfer simulations of neutron star merger ejecta. *Astrophys. J*. **775**, 113. arXiv:1306.3742.

TANAKA, M., UTSUMI, Y., MAZZALI, P. A., TOMINAGA, N., YOSHIDA, M., SEKIGUCHI, Y., MOROKUMA, T., MOTOHARA, K., OHTA, K., KAWABATA, K. S., *et al.* 2017 Kilonova from

post-merger ejecta as an optical and near-infrared counterpart of GW170817. *Publ. Astron. Soc. Jpn* **69** (6), 102. arXiv:1710.05850.

TAVANI, M. 1996 A shock emission model for gamma-ray bursts. II. Spectral properties. *Astrophys. J.* **466**, 768.

TCHEKHOVSKOY, A., MCKINNEY, J. C. & NARAYAN, R. 2009 Efficiency of magnetic to kinetic energy conversion in a monopole magnetosphere. *Astrophys. J.* **699** (2), 1789–1808. arXiv:0901.4776.

TROJA, E., CUSUMANO, G., O'BRIEN, P. T., ZHANG, B., SBARUFATTI, B., MANGANO, V., WILLINGALE, R., CHINCARINI, G., OSBORNE, J. P., MARSHALL, F. E., *et al.* 2007 Swift observations of GRB 070110: an extraordinary X-ray afterglow powered by the central engine. *Astrophys. J.* **665** (1), 599–607. arXiv:astro-ph/0702220.

TROJA, E., VAN EERTEN, H., ZHANG, B., RYAN, G., PIRO, L., RICCI, R., O'CONNOR, B., WIERINGA, M. H., CENKO, S. B. & SAKAMOTO, T. 2020 A thousand days after the merger: continued X-ray emission from GW170817. e-prints. arXiv:2006.01150.

TROJA, E., PIRO, L., RYAN, G., VAN EERTEN, H., RICCI, R., WIERINGA, M. H., LOTTI, S., SAKAMOTO, T. & CENKO, S. B. 2018 The outflow structure of GW170817 from late-time broad-band observations. *MNRAS* **478**, L18–L23.

TROJA, E., PIRO, L., VAN EERTEN, H., WOLLAEGER, R. T., IM, M., FOX, O. D., BUTLER, N. R., CENKO, S. B., SAKAMOTO, T., FRYER, C. L., *et al.* 2017 The X-ray counterpart to the gravitational-wave event GW170817. *Nature* **551**, 71–74. arXiv:1710.05433.

UHM, Z. L. & ZHANG, B. 2014 Fast-cooling synchrotron radiation in a decaying magnetic field and γ-ray burst emission mechanism. *Nat. Phys.* **10** (5), 351–356. arXiv:1303.2704.

USOV, V. V. 1992 Millisecond pulsars with extremely strong magnetic fields as a cosmological source of γ-ray bursts. *Nature* **357** (6378), 472–474.

VIETRI, M. 1996 Magnetospheric interactions of binary pulsars as a model for gamma-ray bursts. *Astrophys. J. Lett.* **471**, L95. arXiv:astro-ph/9609028.

VIGANÒ, D., AGUILERA-MIRET, R., CARRASCO, F., MIÑANO, B. & PALENZUELA, C. 2020 GRMHD large eddy simulations with gradient subgrid-scale model. e-prints. arXiv:2004.00870.

VURM, I. & BELOBORODOV, A. M. 2016 Radiative transfer models for gamma-ray bursts. *Astrophys. J.* **831** (2), 175. arXiv:1506.01107.

WALKER, K. C., SCHAEFER, B. E. & FENIMORE, E. E. 2000 Gamma-ray bursts have millisecond variability. *Astrophys. J.* **537** (1), 264–269.

WEIBEL, E. S. 1959 Spontaneously growing transverse waves in a plasma due to an anisotropic velocity distribution. *Phys. Rev. Lett.* **2** (3), 83–84.

WOLLAEGER, R. T., KOROBKIN, O., FONTES, C. J., ROSSWOG, S. K., EVEN, W. P., FRYER, C. L., SOLLERMAN, J., HUNGERFORD, A. L., VAN ROSSUM, D. R. & WOLLABER, A. B. 2018 Impact of ejecta morphology and composition on the electromagnetic signatures of neutron star mergers. *MNRAS* **478**, 3298–3334. arXiv:1705.07084.

WOOSLEY, S. E. 1993 Gamma-ray bursts from stellar mass accretion disks around black holes. *Astrophys. J.* **405**, 273.

WOOSLEY, S. E. & BLOOM, J. S. 2006 The supernova gamma-ray burst connection. *ARA&A* **44** (1), 507–556. arXiv:astro-ph/0609142.

WU, M.-R., FERNÁNDEZ, R., MARTÍNEZ-PINEDO, G. & METZGER, B. D. 2016 Production of the entire range of r-process nuclides by black hole accretion disc outflows from neutron star mergers. *MNRAS* **463** (3), 2323–2334. arXiv:1607.05290.

XU, S., YANG, Y.-P. & ZHANG, B. 2018 On the synchrotron spectrum of GRB prompt emission. *Astrophys. J.* **853** (1), 43. arXiv:1711.03943.

XUE, Y. Q., ZHENG, X. C., LI, Y., BRANDT, W. N., ZHANG, B., LUO, B., ZHANG, B. B., BAUER, F. E., SUN, H., LEHMER, B. D., *et al.* 2019 A magnetar-powered X-ray transient as the aftermath of a binary neutron-star merger. *Nature* **568** (7751), 198–201. arXiv:1904.05368.

YU, Y.-W., CHENG, K. S. & CAO, X.-F. 2010 The role of newly born magnetars in gamma-ray burst X-ray afterglow emission: energy injection and internal emission. *Astrophys. J.* **715** (1), 477–484. arXiv:1004.1685.

YU, H.-F., DERELI-BÉGUÉ, H. & RYDE, F. 2019 Bayesian time-resolved spectroscopy of GRB pulses. *Astrophys. J.* **886** (1), 20. arXiv:1810.07313.

YU, Y.-W., ZHANG, B. & GAO, H. 2013 Bright 'Merger-nova' from the remnant of a neutron star binary merger: a signature of a newly born, massive, millisecond magnetar. *Astrophys. J. Lett.* **776**, L40. arXiv:1308.0876.

ZALAMEA, I. & BELOBORODOV, A. M. 2011 Neutrino heating near hyper-accreting black holes. *MNRAS* **410**, 2302–2308. arXiv:1003.0710.

ZHANG, B. 2018 *The Physics of Gamma-Ray Bursts*. Cambridge Univeristy Press.

ZHANG, B., FAN, Y. Z., DYKS, J., KOBAYASHI, S., MÉSZÁROS, P., BURROWS, D. N., NOUSEK, J. A. & GEHRELS, N. 2006 Physical processes shaping gamma-ray burst X-ray afterglow light curves: theoretical implications from the swift X-ray telescope observations. *Astrophys. J.* **642** (1), 354–370. arXiv:astro-ph/0508321.

ZHANG, B. & MÉSZÁROS, P. 2001 Gamma-ray burst afterglow with continuous energy injection: signature of a highly magnetized millisecond pulsar. *Astrophys. J. Lett.* **552** (1), L35–L38. arXiv:astro-ph/0011133.

ZHANG, B. & YAN, H. 2011 The internal-collision-induced magnetic reconnection and turbulence (ICMART) model of gamma-ray bursts. *Astrophys. J.* **726** (2), 90. arXiv:1011.1197.

ZRAKE, J., BELOBORODOV, A. M. & LUNDMAN, C. 2019 Subphotospheric turbulence as a heating mechanism in gamma-ray bursts. *Astrophys. J.* **885** (1), 30. arXiv:1810.02228.